

8

The Elongation Cycle

Knud H. Nierhaus

The elongation cycle (parts of previous reviews of the Nierhaus group [1–6] have been integrated in this chapter) is the heart of protein synthesis. Each “heart beat” of the ribosome prolongs the nascent polypeptide chain by a single amino acid. The elongation cycle can be divided into the following three basic reactions: (i) Occupation of the A-site by the incoming tRNA. This step can be further subdivided into (a) the decoding reaction, which mainly restricts the aminoacyl-tRNA and ribosome interactions to codon–anticodon interactions (low-affinity interaction) and (b) the accommodation reaction, where high-affinity binding of the whole tRNA to the A-site results in the docking of the aminoacyl residue into the peptidyl transferase (PTF) center of the large subunit. (ii) Peptide-bond formation, where the nascent polypeptide chain is transferred from the P-site tRNA onto the aminoacyl moiety of the A-site tRNA. This leaves a deacylated (or uncharged) tRNA at the P-site and a peptidyl-tRNA at the A-site (with the nascent chain extended by one amino acid). (iii) Translocation involves the movement of mRNA•tRNA₂ on the ribosome by one codon length so as to place the deacylated tRNA into the E-site and the peptidyl-tRNA into the P-site, thus freeing the A-site for the next incoming aminoacyl-tRNA. Progression of the ribosome through these various stages of the elongation cycle is catalyzed by protein factors called elongation factors, specifically elongation factor G (EF-G) and elongation factor Tu (EF-Tu) in bacteria. These factors transiently interact with the ribosome at specific points during the elongation cycle to facilitate movement onto the following stage of the cycle, e.g., EF-Tu facilitates delivery of the aa-tRNA to the A-site (step 1), whereas EF-G mediates movement or translocation of the tRNAs from the A- and P-sites to the P- and E-sites, respectively (step 3). Translocation shifts the ribosome from a pre-translocational (PRE) state to a post-translocational state (POST). Both factors have been visualized by cryo-EM in functional complexes with the ribosome at various stages during the elongation cycle [7–10]. By combining these reconstructions with those of PRE and POST tRNA•70S ribosome images, a comprehensive overview of the elongation cycle has been constructed from cryo-EM images [11] (Fig. 8-1).

The ribosomal state before translocation (PRE in Fig. 8-1c) is characterized by tRNAs at the A- and P-sites and, following translocation (POST as seen in Fig. 8-1f), by tRNAs at the P- and E-sites. The PRE and POST states represent the main states

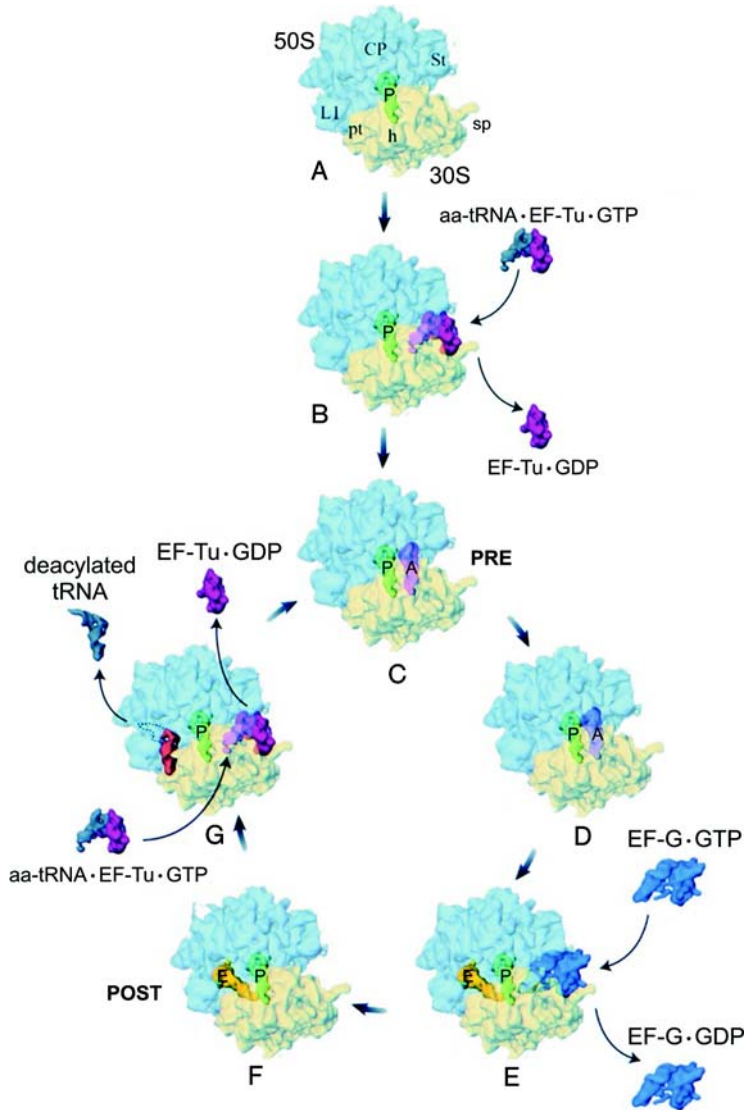


Figure 8-1 Overview of the translation cycle. Multiple cryo-electron microscopic studies have determined the tRNA and elongation factor-binding positions on the 70S ribosome during different stages of the elongation cycle (see Ref. [11] and references therein). These positions of the ribosomal ligands have been overlaid on to an 11.5 Å resolution three-dimensional (3D) map of the ribosome to generate a schematic overview of the elongation cycle, the details of which are provided in the text. The small 30S subunit is in yellow, the 50S large subunit in blue. Adapted from Agrawal et al. [11].

of the active ribosome and are separated by high activation-energy barriers (about 80–90 kJ mol⁻¹; [12]). The POST state probably represents a lower energy level of the ribosome than the PRE state. This is indicated by the fact that after peptide-bond formation an incubation at 37° C for 2 min is sufficient to promote translocation from the PRE to the POST state in the absence of the translocation factor EF-G and GTP (“spontaneous translocation”, [13–15]). In contrast, the reverse translocation has never been observed with an isolated POST state.

Therefore, during the elongation cycle, the ribosome can be thought of as oscillating between the two main states, namely the PRE and POST states. Even ribosomes carrying only a P-site tRNA (e.g., AcPhe-tRNA), a state that is referred to as the P_i state, seems to exist in two different conformations, as evident from the differential effects of puromycin, tetracycline, viomycin, and thiostrepton on the two subpopulations of ribosomes [16]. Finally, even the empty ribosome can adopt two different conformations, one resembling the PRE, the other the POST conformation, as judged by synergistic effects of EF-Tu and EF-G on their respective uncoupled GTPases [17].

By reducing the activation energy barrier that exists between the PRE and POST states, the elongation factors significantly accelerate protein synthesis by more than four orders of magnitude (104-fold; a spontaneous translocation in the absence of EF-G lasts about 2 min [13], and an enzymatic translocation in the presence of EF-G about 30 μs [18]). Therefore, they resemble enzymes which also lower the activation energy of a reaction and, due to the enormous acceleration factor of 10⁶–10¹² achieved, just enable a reaction to occur [19]. But enzymes accelerate a reaction only until the equilibrium is reached, i.e., enzymes can usually catalyze both the forward and reverse reactions. In this respect, the elongation factors are more specific since they not only accelerate the reaction rate but also determine the direction of the reaction: EF-Tu catalyzes the POST→PRE transition and EF-G the reverse PRE→POST reaction. This unidirectional mechanism of action of the elongation factors explains why the presence of two elongation factors is universally conserved. Only the higher fungi such as *Saccharomyces cerevisiae* or *Candida albicans* require a third factor, EF-3, which is essential for protein synthesis playing a role in removal of deacylated tRNA from the E-site of the ribosome ([20]; see Sect. 8.1.2 for the ATP-dependent functions of EF-3).

Both the universal elongation factors are prototypes of the large superfamily of G-proteins. Like all G-proteins, these elongation factors are GTPases and follow a cycle of activation in the presence of GTP (the “ON” conformation) and deactivation when GDP is bound (“OFF” conformation) [21]. In the “ON” or GTP conformation, G-proteins bind to their target substrate, be it a protein or complex, to trigger their specific reaction. Subsequently, the GTPase center of the G-protein is activated and the terminal phosphate residue of the bound GTP molecule is cleaved off to yield GDP. The G-protein now adopts the deactivated “OFF” conformation, which has a lower affinity for the target substrate and therefore dissociates from it. For the cycle to be repeated, GDP must be exchanged for GTP on the G-protein. This means for the elongation factors, the energy liberated by the elongation-factor-dependent GTP

hydrolysis is used for the release of the elongation factors after they have done their job rather than for the reaction triggered by the elongation factors in their “on” state (a different view for EF-G was proposed by the “motor protein” hypothesis; see Sect. 8.4.1).

8.1

Models of the Elongation Cycle

Before we describe the molecular details of the individual reactions of the elongation cycle, we will briefly and critically consider the two prevailing models of the elongation cycle, namely the hybrid site and α - ϵ model.

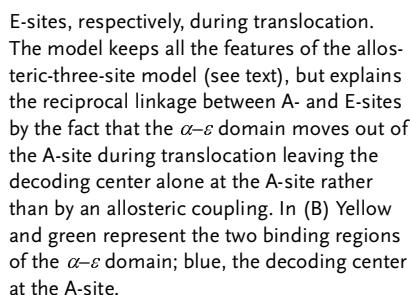
8.1.1

The Hybrid-site Model for Elongation

This model is based on the observation that bases of rRNA were protected against chemical modification when tRNAs were bound specifically to the ribosomal A-, P- and E-sites. Each tRNA position on the ribosome was correlated with a specific protection pattern, e.g., binding of AcPhe-tRNA (a simple mimic of a peptidyl-tRNA) to the P-site defined the “P-site pattern”, whereas binding of a ternary complex Phe-tRNA-EF-Tu-GTP to the A-site (after pre-filling the P-site with a deacylated-tRNA) produced an “A-site pattern”. The “E-site pattern” was derived simply from the binding of deacylated tRNA to the E-site, but was not very well defined in the poly(U)-dependent system used [22].

When AcPhe-tRNA was bound to the P-site and the protection patterns were assessed both before and after “peptide-bond formation” (or more accurately, the transfer of the AcPhe to puromycin in the A-site), the P-site pattern shifted to an E-site pattern on the 23S rRNA after peptide-bond formation, whereas an unaltered P-site pattern remained on the 16S rRNA. The conclusion was that the tRNA was in a P/P state before and in a P/E state after the puromycin reaction (where the letter before and after the slash indicate the site bound by the tRNA on the 30S and 50S subunit, respectively). In another experiment, ternary complex was added to ribosomes carrying an AcPhe-tRNA at the P-site, which following peptide-bond formation would put an AcPhe-Phe-tRNA at the A-site and a deacylated tRNA at the P-site. An “A plus P” pattern was observed on the 16S rRNA, whereas the 23S rRNA exhibited a “P plus E” pattern. These results were interpreted such that the analog of the peptidyl-tRNA was in an A/P-site and the deacylated tRNA in a P/E site. Following translocation, the protection patterns suggested that the tRNAs were in the P/P and E-sites, where the E-site is located solely on the 50S subunit rather than on the 30S subunit.

The hybrid-site model [22] in its original form is depicted in Fig. 8-2(A) with its diagnostic feature of hybrid sites after peptide-bond formation: the tRNAs pass through the ribosome with a “creeping” movement. On the 30S the picture follows the classical scheme outlined in the preceding section; however on the 50S, the



movement is proposed to start *after* peptide-bond formation but *before* EF-G-dependent translocation. The model has been modified in light of the crystal structure [23], where the E-site tRNA shows intensive contacts with the small subunit, such that now the tRNA is found in the E/E-site after translocation [24]. A further change was introduced so that after peptide-bond formation the tRNAs initially remain at the classical A/A- and P/P-sites, before they shift, after an undefined time period, into the hybrid A/P- and P/E-sites, respectively [24]. These changes were necessary to account for the observation that no hybrid sites were observed in a systematic study of the elongation cycle ([11]; also see below) and the CCA ends did not move after peptide-bond formation in a 50S crystal [25].

In functional studies, the P-site is operationally defined as the site where an acylated-tRNA can react with puromycin, in contrast with an A-site location where it is for all intense and purposes puromycin unreactive. The observation that an acylated tRNA can in fact undergo the puromycin reaction [26] does not seriously challenge this definition, since the latter reaction differs qualitatively from that of the P-site reaction in that it is extremely slow. For example, under conditions of 6 mM Mg^{2+} and in the presence of polyamines, the A-site puromycin reaction proceeds 200 times slower than that in the P-site (A. Potapov, C. Spahn and K. H. Nierhaus, unpublished results). Note that the hybrid-site model uncouples the functional definition of the P-site from the structural one, because this model locates the peptidyl residue at the P-site of the PTF center (on the 50S subunit) after the peptide-bond formation (because the peptidyl-tRNA is at the A/P-site), yet the peptidyl residue is not puromycin-reactive. Consequently, this model is forced to distinguish between two P-site positions on the 50S subunit, one that is puromycin-reactive and one that is not. Finally, the problem of moving the $(tRNA)_2 \cdot mRNA$ complex has not become significantly simpler, even though the tRNA movement from one site to the other now occurs in two steps.

There are two major criticisms that should be considered when applying the hybrid-site model:

1. The concept of hybrid sites rests solely on the protection patterns of the 23S rRNA. However, the protections of 16 out of 17 bases of 23S rRNA were dependent on the ultimate A_{76} residue or $CA_{76-3'}$ residues of the universal CCA-3' terminus of the tRNAs [27]. In contrast with the hybrid-site perception, the crystal structure of the 50S subunit after peptide-bond formation demonstrates that the CCA ends at A- and P-sites do not move [25].
2. The experiments from which the model is derived employs a vast range of Mg^{2+} concentrations ranging from 5 to 25 mM [28, 27]. However, it is well known that the binding properties and the interdependencies of the various sites are extremely sensitive to changes in Mg^{2+} concentration [29]. This sensitivity probably reflects an increasing distortion of the ribosome with increasing Mg^{2+} concentration, which one would expect affects a fine-structure analysis such as the chemical probing of the rRNA bases. In fact, a deacylated tRNA bound to programmed ribosome under conventional ionic conditions (Table 8-1) was found exclusively at the P/E hybrid site, whereas under more *in vivo* ionic conditions, the deacylated tRNA was

found at the classical P-site, suggesting that the hybrid-site concept may simply be a buffer artefact [30]. A systematic analysis of tRNA-binding sites during elongation did not provide any evidence for hybrid states of a tRNA [11]. Recently, cryo-EM of PRE state ribosomes prepared in a different laboratory also showed no evidence for the presence of hybrid states [31]. In this study, the post-peptide-bond formation of PRE state ribosome complexes had a dipeptidyl tRNA at the classical A-site and not at the A/P hybrid site as would be predicted by the hybrid-site model. From these independent studies, it is at least clear that a ribosome containing a hybrid site does not represent a significant proportion of the elongating ribosome population. Furthermore, the crystal structure of a programmed ribosome containing three deacylated tRNAs at 5.5 Å resolution identified a deacylated tRNA at the classical P-site [23], rather than at the P/E hybrid site as might be expected from the hybrid-site model.

Contrary to the belief of some, the ratchet model, where the subunits twist relative to each other in a forward-and-back movement by about 4.5° during translocation [32], does not in fact support the hybrid-site model. This is because the forward-and-back ratchet movements occur *during* one translocation step, i.e., the tRNAs are at A- and P-sites before translocation and at P- and E-sites after translocation (see Sect. 8.4.2). However, it could be that during one translocation reaction the two tRNAs do transiently pass through a hybrid position when they go from the A- and P-sites to the P- and E-sites, respectively. In fact, this interpretation is supported by a cryo-EM analysis of the translocation movement [31], suggesting that hybrid states are indeed translocation intermediates.

8.1.2

The Allosteric Three-site Model (α - ϵ Model; Reciprocal Coupling between the A- and E-sites)

Under unfavorable buffer conditions the dissociation rate of a tRNA at the E-site was reported to be 0.3 s⁻¹ [33], whereas the elongation rate, determined under comparable conditions, was reported to be 10 times faster (3 s⁻¹) [34]. This alone suggests that an active mechanism must exist to eject the deacylated tRNA from the E-site. Under near *in vivo* conditions, the situation is even more significant: the dissociation rate of an E-site tRNA from an isolated POST state is much lower and can be measured in hours rather than seconds. POST states can be isolated via overnight centrifugation through sucrose cushions without loss of any deacylated tRNA from the E-site (see, e.g., Ref. [35]), and native polysomes isolated using a procedure lasting longer than 24 h contain an occupied E-site almost quantitatively [36]. It is clear that the release of a deacylated tRNA from the E-site must be an active process and cannot occur via a simple diffusion process as considered by some authors (see, e.g., Ref. [37]). In fact, crystal structures of 70S•tRNA complexes [23] and cryo-EM studies [31] have demonstrated stable and tight E-site binding, although a mechanism for the E-tRNA release was not deduced.

A reciprocal linkage between A- and E-sites has been identified as being the active mechanism for E-site ejection: the E-site affinity drops markedly upon occupation of the A-site and *vice versa*, i.e., the occupation of the A-site is coupled with the tRNA

release from the E-site [38, 39]. In the years following the identification of the reciprocal linkage between A- and E-sites, much data accumulated providing support for this model: (i) A direct and unequivocal demonstration of the reciprocal linkage was achieved using a heteropolymeric mRNA displaying three different codons at the three sites together with three respective cognate tRNAs, each labeled with a different isotope [40]. (ii) The activation energy for occupation of the A-site depends on the charging state of the E-site: when a tRNA is present at the E-site the activation energy is twice as large as that observed when the E-site is free [12]. (iii) Thiostrepton, viomycin and all types of aminoglycosides severely impair A-site binding only if the E-site is occupied [41]. (iv) The reciprocal coupling of A- and E-sites has also been observed with the ribosomes of organisms from other evolutionary domains, viz. with ribosomes of *Halobacterium halobium* (archaea; [42]) and yeast (eukarya; [20]), suggesting that this relationship is universally conserved. Indeed, in yeast, the reciprocal coupling was observed when the functions of the third elongation factor (EF-3) were studied [20]. In the POST state, yeast 80S ribosomes bound the E-tRNA so tightly that a ternary complex aa-tRNA•EF-1•GTP could not bind to the A-site. First, the binding of EF-3 to the ribosome and ATP cleavage was necessary to free the E-site tRNA, perhaps by “opening” up the E-site by movement of the L1 protuberance of the 50S subunit. Only then was it possible for A-site occupation and the concomitant release of the E-tRNA to occur. These results illustrate the bi-directionality of the reciprocal linkage: if the E-tRNA cannot be released, the A-site remains in its low-affinity state and cannot be occupied; if EF-3 “opens” the E-site, A-site occupation triggers release of the E-tRNA.

The reciprocal linkage between A- and E-sites led to the “allosteric three-site model”, which is characterized by three basic features (the last version is the α - ϵ model, see Fig. 8-2B; see Ref. [43] for review):

1. Ribosomes contain three tRNA-binding sites [44, 45].
2. The first and the third sites, A- and E-sites, respectively, are coupled in a reciprocal fashion: occupation of the A-site decreases the affinity at the E-site and *vice versa* [40, 39, 20].
3. Both tRNAs that are present at the A- and P-sites before translocation and at the P- and E-sites after translocation are linked to the mRNA via codon–anticodon interaction [46, 20]. Codon–anticodon interaction at the E-site seems to be essential for establishing the POST state containing the P- and E-tRNAs [47]. Only the POST state is the proper substrate for the ternary complex aa-tRNA•EF-Tu•GTP.

The reciprocal linkage model was extended to the so-called α - ϵ model when the accessibility of the phosphate groups of a tRNA at the various ribosomal sites was tested in PRE and POST states. These experiments demonstrated that a tRNA in the A-site of a PRE state ribosome had a strikingly different pattern when compared with the corresponding tRNA in the P-site [48]. However, after translocation to the P- and E-sites, the protection patterns of both tRNAs hardly changed [49]. The conclusion was that the tRNAs bound to a structural domain of the ribosome, and that this structural domain moved during translocation from the A- and P-sites to the P- and E-sites while maintaining contact with both tRNAs. Therefore, the structural

domain was considered to contain two binding regions, which were termed α and ε (Fig. 8-2B). A tRNA bound to the α binding region is located at the A-site before translocation and at the P-site after translocation. Similarly, a tRNA bound to ε binding region is located at P-site before translocation and at the E-site after translocation. Thus, only α can appear at the A-site and only ε at the E-site (hence the nomenclature), whereas at the P-site either α or ε can be present depending on the translocation state. Support for the model was recently provided by results obtained using a completely different approach: site-specific Pb²⁺ cleavage was applied to trace tertiary alterations of tRNAs and rRNAs in PRE and POST state ribosomes [50]. Deacylated tRNAs and AcPhe-tRNA produced the same cleavage pattern in solution but very different ones when bound to the ribosome. Consistent with phosphorothioate experiments, the specific and distinct patterns for the bound tRNAs did not change during translocation. This again led to the conclusion that while the tertiary structure of the adjacent tRNAs at A- and P-sites are different, the fact that they do not change during translocation argues for a ribosomal “conveyor” that binds both tRNAs and moves them during translocation. Comparing contact patterns of tRNAs obtained with isolated subunits and 70S ribosomes using the phosphorothioate method indicated that the two parts of the “conveyor”, both of which bind a tRNA, probably move in a concerted fashion but not strictly side-by-side [51]. Therefore, the recent observation that the deacylated tRNA seems to move from the P- to the E-site via a hybrid position [31] is not in conflict with the α - ε model.

The α - ε model integrates the well-documented fact that the post-translocational ribosome with a low-affinity A-site is capable of selecting the aminoacyl-tRNA cognate to the codon at the A-site, i.e., the decoding process occurs before the α - ε domain of the ribosome flips back from the P-E-site to the A-P-site. According to the α - ε model, the decoding site, being exclusively on the 30S subunit, is stably located at the A-site where it is called δ . It follows that α is superimposed on δ in the PRE state and separated from the δ domain in the POST state (Fig. 8-2B). This feature of the α - ε model predicts that the ribosome has two tRNA-binding sites in the PRE state and three in the POST state (the two high-affinity sites α - ε at the P- and E-sites and the low-affinity site δ at the A-site).

All three features of the allosteric three-site model are also valid for the α - ε model, although they are extended or re-interpreted, such that (i) the three tRNA-binding sites still exist but only in the POST state. Saturation of 70S ribosomes with deacylated tRNAs levels off at three tRNAs per ribosome. First, the P- and E-sites are filled, thus establishing a POST state, thereby creating a low-affinity A-site (δ -site at the A-site). This is illustrated by the requirement of excess (> 6-fold) of deacylated tRNAs over ribosomes to fill the third site [45]. (ii) The A- and E-sites have an inverse relationship in that an occupied E-site is accompanied by a low-affinity δ -site at the A-site and an occupied A-site with no affinity at the E-site. The new interpretation of this relationship is that allostery is not involved: during translocation the α region moves from the A-site to the P-site leaving the decoding center δ in the A-site (“low-affinity” A-site), and during aminoacyl-tRNA binding to the A-site the α - ε domain jumps from the P-E to the A-P, leaving the E-site without a tRNA-binding capacity. (iii) The

two tRNAs have a similar mutual arrangement relative to each other. In fact, the angles between the tRNAs in the PRE and POST states are almost identical, as shown by cryo-EM analysis (39° and 35° in the PRE and POST states, respectively [11]). Also the arrangement relative to the mRNA, i.e., the codon–anticodon interactions, is maintained before, during and after translocation with regard to the α – ε binding regions. Thus, the movement of the tRNAs occurs simultaneously on the two subunits in a coordinated fashion, and during translocation the tRNAs might transiently move through hybrid positions as has been made evident for the deacylated tRNA moving from the P-site over the hybrid position P/E to the E-site [31], whereas the predictions of the hybrid-site model, namely that the tRNAs swing into a hybrid site after peptide-bond formation could not be confirmed [11, 31]. However, the CCA ends of the two tRNAs present at A- and P-sites are directly adjacent at the PTF center at the PRE state (required for peptide-bond formation), whereas they are separated substantially in the POST state. After the peptide bond has been formed, there is no need to keep them together (see Figs. 6-2A and B in Chap. 6). This fact indicates that the α and ε regions do not strictly move side-by-side during translocation.

Ribosomal candidates for a movable domain have been identified as bridge B2a in 70S ribosomes via cryo-EM [52] and X-ray crystallography [23], and probable ribosomal components such as the upper region of the h44 of the 16S rRNA [53], H69 of the 23S rRNA and parts of the ribosomal protein L2 [54, 55].

The α – ε model provides a dynamic picture of the translating ribosome. The translocation reaction is explained in a (possibly too) simple fashion: the α – ε domain moves together with both tRNAs and the corresponding codons. The required movement of about 10 Å, the length of a codon, is not unusual for molecular movements of enzyme substructures. For example, the distance between the first and the second domains of EF-Tu is enlarged by up to 40 Å upon GTP cleavage [56]. According to the α – ε model, the critical step during the elongation cycle is not the translocation reaction but rather the binding of the new aminoacyl tRNA in the α -site at the A-site, since during the latter the α – ε domain has to release the tRNAs in order to switch from the E-A-sites to the P-A sites (see Fig. 8-2B). This is in agreement with the finding that occupation of the A-site is the rate-limiting step of elongation, not the translocation reaction [57, 12].

To date, the most comprehensive analysis of the translocation reaction by cryo-EM [31] challenges an essential feature of the α – ε model, namely, PRE state ribosomes carrying an fMet-Phe-tRNA at the A-site and a deacylated tRNA^{Phe} at the P-site, also carried a tRNA at the E-site. This was particularly surprising since deacylated tRNA was not actually included in the reaction; however, the authors assumed that the source of the E-tRNA was the free pools of deacylated tRNA in solution, which enabled direct binding to the “high-affinity” E-site. Regardless of the source, the presence of simultaneously occupied A- and E-sites is in direct contradiction with the α – ε model. However, to contradict the α – ε model directly the stoichiometry of the A- and E-sites needs to be assessed. The authors made no attempts to resolve this conflict between their conclusions and the findings that an E-site release upon A-site occupation has been observed with both prokaryotic and eukaryotic ribosomes

(see Ref. [58] for review). In any case, it is clear that we are far from having a detailed picture of the translocation reaction and the presence of high-resolution structures of PRE and POST states would certainly go some way to resolving one of the central enigmas of ribosome research.

8.2

Decoding and A-site Occupation

8.2.1

Some General Remarks about Proofreading

The term “proofreading” stems from the glossary of the printing arts. The first out-print of a newspaper, e.g., was checked by the print master, and if he found a misprint, the letter was exchanged and the mistake corrected for the second print that was delivered to the clients. In molecular biology, this term has a similar meaning, in that the last amino acid building block that is to be added to the growing polypeptide chain is checked for correctness before it is permanently incorporated into the synthesized protein.

Proofreading is a common phenomenon in polymerases that synthesize DNA [59] and RNA [60]. In fact, polymerization of nucleic acids is well suited for proofreading, since its basic mechanism is that of “tail growth” (Fig. 8-3). This means the new building block that is to be added to the nascent chain is providing the energy-rich bond (the phosphoric acid anhydride bond between the α and the β phosphate residues of an NTP) for the link (the 3' ester bond) to the nascent chain. If the addition was wrong, the proofreading center hydrolyzes the last four nucleotides, thus enabling another chance for the correct addition.

In contrast, the situation is very different in the case of protein synthesis since it follows the principle of “head growth” (Fig. 8-3): the nascent chain provides the energy-rich ester bond for the formation of the peptide bond that links the newly added amino acid. The peptidyl residue is added to the newly arrived amino acid, and the ester bond of the latter is used for the next round of elongation. Therefore, in *strictu sensu*, proofreading cannot exist in protein synthesis, since such a process would sacrifice the already synthesized chain via removal of the last incorporated amino acid. Not surprisingly, therefore, a “proofreading center” was not detected in the atomic structures of the ribosome. Nevertheless, the term proofreading is widely used in the field of protein synthesis, but here in a broader sense, such as “kinetic proofreading” that will be discussed in Sect. 8.2.3. We should also note here that synthetases of both class I and class II have “proofreading centers” that play an important role for achieving the accuracy of charging tRNAs [61–63] (see also Chap. 4.2).

8.2.2

Discrimination against Noncognate aa-tRNAs

A new elongation cycle begins when an aa-tRNA enters the ribosomal A-site as the ternary complex aa-tRNA·EF-Tu·GTP. The codon displayed in the A-site is specific

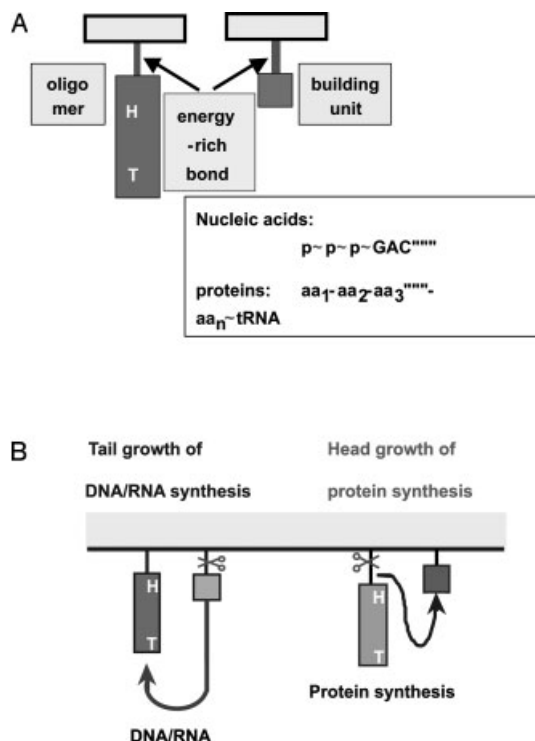


Figure 8-3 Principles of tail- and head-growth: (A) Definitions of head (H) and tail (T) in the synthesis of nucleic acids and proteins. Tail growth means that the energy-rich bond of the new building unit is used for incorporation, whereas during head growth the energy-rich bond of the nascent chain is used for incorporation of a new building block. (B) Tail growth is exemplified by the synthesis of nucleic acids (activities of replicases and transcriptases), and head growth to protein synthesis on the ribosome. See text for details.

for a single species of tRNA, termed the *cognate* tRNA, which has an anticodon that perfectly complements the A-site codon. However, there are many other tRNA competitors that can interfere with this selection process: 41 in *E. coli* and even more in the eukaryotic cell. To make matters worse, 4–6 of these tRNAs, termed *near-cognate* tRNAs, will have an anticodon similar to the cognate tRNA. The remaining 90% have a dissimilar anticodon and are termed *noncognate* tRNAs. The problem is compounded further when one considers that the aa-tRNAs are delivered in the form of a ternary complex, i.e., in complex with the elongation factor EF-Tu and GTP. The ribosome must therefore discriminate between relatively large ternary complexes (72 kDa), which present multiple potential interaction sites with the ribosome, on the basis of a small discrimination area, the anticodon (1 kDa). The discrimination

potential of the discrimination energy can only be reached under equilibrium conditions and, in this case, the free energy of binding is relatively large, with only a tiny fraction being discrimination energy. This means that equilibrium can only be reached after long time periods, i.e., this process must be slow to be accurate. Since we know that protein synthesis is a relatively fast and accurate process, the ribosome must overcome this hurdle. The question is how?

A model has been proposed which overcomes this problem by simply dividing A-site occupation into two distinct events; a decoding step followed by an accommodation step (reviewed in Ref. [64]). During the initial decoding step, the A-site is in a low-affinity state, which reduces interaction of the ternary complex to mainly codon–anticodon interactions, thus excluding general contacts of the tRNA and elongation factor. By restricting the binding surface of the ternary complex to the discriminating feature, i.e., the anticodon, the binding energy is both small and equivalent to the discrimination energy. In addition, since the binding energy is small, equilibrium can be rapidly attained, thus ensuring the efficiency of the reaction is retained. The second step, accommodation of the A-site, requires release of the aa-tRNA from the ternary complex into the A-site. This step utilizes the nondiscriminatory binding energy to dock the tRNA precisely into the A-site and the attached amino-acyl residue into the PTF center on the 50S subunit in preparation for peptide-bond formation. As we have already seen in the previous section, accommodation of the aa-tRNA in the A-site is accompanied by release of the E-tRNA. Evidently, this second step of A-site binding involves gross conformational changes within the ribosome [12] and thus can be thought of as a relatively slow process in comparison with the first or decoding step. It follows that A-site binding occurs via a coupled reaction system, consisting of a fast initial decoding and a slow second accommodation reaction. This has the important consequence that the initial reaction operates at equilibrium even when the whole system runs under steady-state conditions. It is this feature that enables the discriminatory potential of codon–anticodon interaction to be efficiently exploited.

Recently, the first step of A-site binding (low-affinity A-site) was viewed using cryo-EM by analyzing ternary complexes stalled at the A-site using the antibiotic kirromycin [65, 10]. Although kirromycin allows GTP hydrolysis, it inhibits the associated conformational changes in EF-Tu that are necessary for dissociation from the ribosome. The cryo-EM reconstructions suggest that the anticodon-stem loop of the tRNA is kinked to allow codon–anticodon interaction and thus overcomes the unfavorable incoming angle of the tRNA to the A-site dictated by the ternary complex (see Fig. 8-4; [10]).

As accommodation of an aa-tRNA into the A-site involves the dissociation of EF-Tu-GDP from the ribosome, which is in turn coupled with the hydrolysis of GTP, it is interesting to note that in *E. coli* up to 2 GTPs are hydrolyzed during the incorporation of cognate-tRNAs and up to 6 for near-cognate-tRNAs, whereas noncognate-tRNAs do not trigger EF-Tu-dependent GTP hydrolysis at all [66]. The acceptance of a near-cognate aminoacyl-tRNA consumes three times more GTP than that of a cognate one, thus improving the accuracy by a factor of 3 only. Since the total

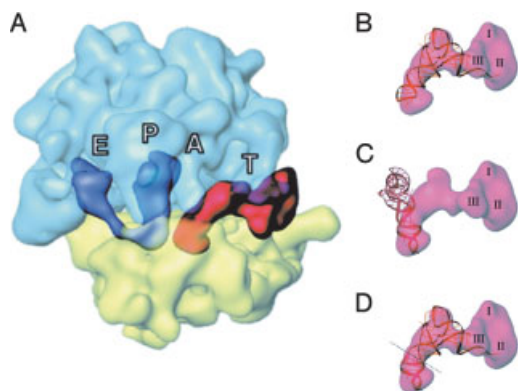


Figure 8-4 The ternary complex on the ribosome during the decoding process. (A) Binding of the ternary complex aa-tRNA•EF-Tu•GTP (red or pink) during the first step of A-site occupation (T position), with tRNAs present at P- and E-sites. Ribosomal subunits are in blue (large subunit) and yellow (small subunit). (B-D) Fitting of the crystal structure of the ternary complex into the difference mass corresponding to the ternary complex on the ribosome. To fit satisfactorily the crystal structure of a tRNA into the corresponding cryo-EM density requires the introduction of a kink in the anticodon stem of the amino-acyl-tRNA of about 40°. From Ref. [10]; for details see text.

accuracy is characterized by a factor of about 3000 (one mis-incorporation in 3000 incorporation events), it is clear that this observation adds further weight to the argument that the tRNA discrimination is governed predominantly by anticodon–codon recognition during the initial binding step (see also the next section).

Why is the low-affinity A-site during the decoding step important for preventing the interference of noncognate tRNAs with the decoding reaction? Preventing this interference by noncognate tRNAs is not trivial since they represent the majority of about 90% of the ternary complexes. If the decoding step reduces the interactions of the ternary complex with the ribosome mainly to codon–anticodon interaction, then this will prevent noncognate ternary complexes interfering with decoding, since interaction of the ternary complex outside of the anticodon is not possible and the anticodon of noncognate tRNAs cannot form efficient base-pairs with the codon displayed at the A-site. In other words, the A-site codon does not really exist for the noncognate complexes. This fact reduces the selection problem by an order of magnitude: instead of selecting one out of 41 tRNA species (cognate versus near- plus noncognate tRNAs) only 1 out of 4–6 tRNAs have to be selected (cognate versus near-cognate tRNAs). The selection problem is comparable with that of a transcriptase selecting the correct nucleotides out of 4 possible ones during RNA synthesis. This process occurs with a precision of better than one mistake in 60 000 incorporations without proofreading [60]. The fact that the noncognate ternary complexes do not interfere with the selection process has been demonstrated by a number of different

approaches: (i) When an E-tRNA induces a low-affinity A-site, a noncognate ternary complex is not incorporated into the nascent peptide chain [47]. (ii) The addition of an excess of noncognate ternary complexes does not slow down the rate of poly(Phe) synthesis in fast systems ([67] and A. Bartetzko and K.H. Nierhaus, unpublished observations). (iii) As mentioned previously, noncognate ternary complexes also show no traces of GTP turnover, whereas near-cognate complexes have a turnover about three times higher than that of cognate ternary complexes [66].

The next obvious question is how the cognate and near-cognate tRNAs are discriminated. This is a question that can now be answered at the molecular level, as discussed in the next section.

8.2.3

Decoding of an aa-tRNA (Cognate versus Near-cognate aa-tRNAs)

A model for the discrimination between cognate and near-cognate aa-tRNAs was proposed by Potapov about 20 years ago [68]. According to this model, the decoding center of the ribosome recognizes the anticodon–codon duplex, in particular sensing the stereochemical correctness of the partial Watson–Crick base-pairing and the positioning of the phosphate-sugar backbone within this structure. A test of this hypothesis was performed with an mRNA that carried a DNA codon (deoxycodon) at one of the three ribosomal sites. If the stability of the base pairs, i.e., the hydrogen bonding between codon–anticodon bases of the Watson–Crick pairs, is the sole requirement for the recognition step, then a 2'-deoxy base in the codon should not affect the decoding process. If, however, the stereochemical correctness of the base pairing is tested, i.e., including the positioning of the sugar pucker, then a 2'-deoxy base should impair the decoding process. It was found that a deoxycodon at the A-site was disastrous for tRNA binding at this site, whereas a deoxycodon at the P-site had no effect on tRNA binding to the P-site. This observation also explains previous results according to which a DNA cannot take over the function of an mRNA (see Ref. [69] and references therein).

The components of the ribosome directly involved in decoding were identified to 3.1 Å by crystallography [70]. Crystal packing of the *Thermus thermophilus* 30S subunit fortuitously placed the spur (h6) of one subunit into the P-site of another, thus mimicking the anticodon stem loop (ASL) of a P-tRNA. Another surprise was that the base-pairing partner to the P-tRNA mimic was the 3'-end of the 16S rRNA, which folding back on itself extended into the decoding center. This situation, with the P-site filled, enabled Ramakrishnan and co-workers [70] to soak an ASL fragment (ASL-tRNA) and a complementary mRNA fragment into these crystals to study aa-tRNA decoding at the A-site.

The results can be summarized as follows: the binding of mRNA and cognate aa-tRNA induces two major rearrangements within the ribosomal decoding center: the universally conserved residues A1492 and A1493 flip out of the internal loop of h44, whereas the universally conserved base G530 switches from *syn* to *anti* conformation. A1493 recognizes the minor groove of the first base pair (ASL-tRNA position A36–U1 of the mRNA) via a type I A-minor motif (Fig. 8-5A). A1493 establishes

three hydrogen bonds (H-bonds) with the first position of the codon–anticodon duplex: two with 2'-OH groups from both A36 and U1 and another with the O2 of U1. It is noteworthy that the latter H-bond is not sequence-specific as might be expected, since the O2 position of pyrimidines and the N3 of purines occupy equivalent positions in the minor groove of a double helix and both are H-bond acceptors.

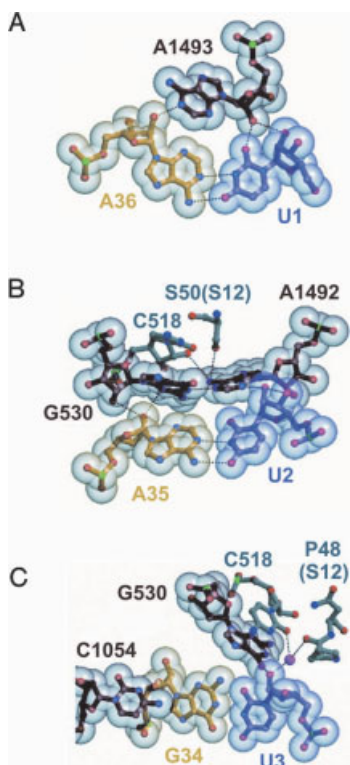


Figure 8-5 The principles of decoding in the A-site of the ribosome. (A) The first base pair of codon–anticodon interaction (position 1) exemplifies a type I A-minor motif: A1493 binds to the minor groove of the A36–U1 base pair via H-bonds. (B) The middle position illustrates a type II A-minor motif: A1492 and G530 acting in tandem to recognize the stereochemical correctness of the A35–U2 base pair using H-bonds. (C) The third (or wobble) base pair (G34–U3) is less rigorously monitored. C1054 stacks against G34, whereas U3 interacts directly with G530 and indirectly with C518 and proline 48 of S12 through a magnesium ion (magenta). All nucleotides involved in monitoring positions 1 and 2 are universally conserved. Adapted from Ogle et al. [70].

The second base pair (A35–U2) is also monitored via 2'-OH interactions, but the job is split between two bases, namely A1492 and G530 (this type II interaction of an A-minor motif is seen in Fig. 8-5B). A1492 and G530 are locked in position by secondary interactions with S12 (serine 50) and another universally conserved residue, C518. Monitoring the second base pair seems to occur more rigidly than that of the first pair in accordance with the fact that the second base pair is of utmost importance for decoding followed by the first pair, whereas the third pair of the codon–anticodon duplex is of least importance [71]. In other words, correct positioning of the 2'-OH groups of the first and second base pairs is critical in forming A-minor interactions and thus efficient duplex sensing. In contrast, the third position is less rigorously monitored, allowing latitude for wobble interactions (Fig. 8-5C). This is evident in the third base pair (G34–U3), where the minor groove remains exposed despite direct interactions with C1054, G530 and indirect metal-mediated interactions with C518 and proline 48 of S12. Taken together, these results confirm the Potapov hypothesis and explain how decoding operates through the recognition of the correct stereochemistry of the A-form codon–anticodon duplex. Furthermore, the fact that the components involved are universally conserved suggests that the mechanism of decoding is probably similar for ribosomes from all kingdoms.

Important extensions to this picture could be made when the known crystal data of *T. thermophilus* 30S subunit showing cognate codon–anticodon interactions between an UUU codon and an ASL structure of the tRNA^{Phe} [70] was complemented with a data set obtained after soaking the programmed 30S subunits with near-cognate ASLs from tRNA₂^{Leu} and tRNA^{Ser}. The cognate tRNA^{Phe} has the anticodon 3'-AAG-5', the near-cognate tRNA₂^{Leu} and tRNA^{Ser} contain the anticodons 3'-GAG-5' and 3'-AGG-5' with a G:U mismatch at the first or second position, respectively, whereas such a mismatch is allowed at the wobble position [72]. The most important conclusion from this work was that only the cognate codon–anticodon interaction could induce a “closed” form of the 30S subunit involving a movement of the shoulder and head towards each other, whereas near-cognate ASLs could only induce this conformation in presence of the misreading-inducing aminoglycoside antibiotic pactamycin. The complete movement can be seen under <http://www.cell.com/cgi/content/full/111/5/721/DC1>, and has a number of important consequences. Various nonpolar interactions between the ribosomal proteins S4 and S5 are broken upon transition from the closed to the open form, whereas h44, h27 and S12 come together and can form additional salt bridges (between residues K57 and the phosphate of C1412 of h44 or K46 and the phosphate of A913 of h27). It has already been noted previously that mutations which would be predicted to break the nonpolar interactions between S4 and S5 induce a “ram” phenotype (ram, ribosomal ambiguity mutations: ribosomes with a defect that is characterized by a high-level amino acid mis-incorporation [73, 74]). In other words, these mutations facilitate the transition into the open form and thus reduce translation fidelity by inducing mis-incorporation. On the other hand, mutations of S12 that destabilize the closed form would impair the transition to the closed form and thus increase the fidelity of aa-tRNA selection at the A-site. In fact, mutations of K57 of S12 result in the most-

accurate (“hyperaccurate”) phenotype known. Therefore, we have gained for the first time a molecular understanding of mutants that increase or decrease the level of mis-incorporations of the ribosome. Since an occupied E-site that has been shown to induce a low affinity of the A-site and improve the accuracy (see Ref. [75] for review), also makes an important contribution to the ribosomal power for A-site tRNA discrimination, this suggests that in the frame of the open-closed model of Ramakrishnan and coworkers [72], the extensive contacts the E-site tRNA with both the 30S and 50S subunit might increase the energetic costs for the transition from the open to the closed form.

Prior to the Potapov hypothesis, it had been proposed that the ribosome utilized a “proofreading mechanism” to improve the accuracy of translation [76, 77]. This mechanism was suggested to operate by re-selection of the correct substrate during a so-called “discarding step”, after the initial binding of the A-tRNA. Because re-selection is dependent upon release of the tRNA from EF-Tu and is accompanied by GTP cleavage, the GTP consumption for the incorporation of a cognate and near-cognate amino acid provides a measure of the power of proofreading. Insofar as the crystal structure of EF-Tu and the ribosome are concerned, the ribosomal proofreading mechanism lacks its own active center (see Sect. 8.2.1 for a principal comparison of the synthesis of nucleic acids and proteins concerning proofreading). Instead, the term “proofreading” has been broadened by introducing “kinetic proofreading” that occurs after the release of the binary complex EF-Tu·GDP [78]. A simple model for kinetic proofreading is the following: the binding energy during the decoding step (first step of A-site binding, see 8.2.2) is for the near-cognate aa-tRNA lower than for the cognate one. Therefore, the probability of triggering the gross-conformational change required for the accommodation of the aa-tRNA into the A-site (second step of A-site binding) is lower than for the near-cognate. This in turn prolongs the resting time of the near-cognate aa-tRNA at the low-affinity A-site and provides an additional chance for the near-cognate aa-tRNA to fall off the low-affinity A-site [79] thus increasing the accuracy. Re-binding of this near-cognate aa-tRNA is unlikely in the presence of competing ternary complexes that have a 2–3 orders of magnitude higher affinity for the A-site than the naked aa-tRNA [80].

The importance of the kinetic proofreading step can be quantitatively determined by taking advantage of the fact that the kinetic proofreading mechanism requires EF-Tu-dependent GTP hydrolysis. Accuracy of aa-tRNA selection in the presence of EF-Tu and a noncleavable GTP analog was determined to be 1:1000 [81], an accuracy only three times lower than that seen *in vivo* (1:3000). Exactly a threefold difference was also determined for the GTP consumption per incorporation of cognate versus near-cognate amino acids [66]. Thus it is clear that the significant contribution to the accuracy of translation (1000-fold) lies within the stereo-chemical monitoring of the codon–anticodon duplex by the ribosome as predicted by Potapov and that the “kinetic proofreading mechanism” plays only a minor role, conferring a 3-fold improvement in the accuracy. This view was qualitatively confirmed by a recent direct measurement of the discrimination power of the initial binding without proofreading, where the binding of cognate and near-cognate ASL-tRNA fragments

to the A-site of 70S ribosomes were compared. The accuracy was found to be between 1 : 350 and 1 : 500, thus also demonstrating that the lion's share of the ribosomal accuracy is carried by the initial binding [72].

8.2.4

Roles of EF-Tu

The following functions of EF-Tu can be distinguished: (i) EF-Tu within the ternary complex aa-tRNA•EF-Tu•GTP reduces the activation energy barrier between the POST and the PRE states by about 120 kJ mol⁻¹ [12] and thus allows the transition from the POST to the PRE state with a high rate. (ii) EF-Tu binds an aa-tRNA at the amino acid acceptor stem thus shielding the labile ester bond between the aminoacyl residue and the tRNA. (iii) A third function (related to function (i) but not identical) is the carrier role of EF-Tu, namely, to deliver the aa-tRNA to the A-site: the ternary complex has an affinity for the A-site, 2–3 orders of magnitude higher than that of the corresponding aminoacyl-tRNA [80]. (iv) Another role for EF-Tu was identified by Uhlenbeck and co-workers [82]. Measuring the affinities of various cognate aa-tRNA (e.g., Val-tRNA^{Val}) and some mis-pairs (e.g., Ala-tRNA^{Val}) they recognized that either the amino acid or the tRNA binds to EF-Tu with high affinity to form stable ternary complexes aa-tRNA•EF-Tu•GTP. For example, EF-Tu•GTP easily forms a ternary complex with Asp-tRNA^{Asp} or Asn-tRNA^{Asn}, but not with the mis-charged Asp-tRNA^{Asn}, since in the latter case both moieties bind with low affinities. This observation explains an important scenario that was an enigma hitherto: in most organisms there are only 18 or 19 synthetases, i.e., not the 20 different synthetases corresponding to the 20 natural amino acids. For example, many organisms do not contain a synthetase specific for asparagine (AsnRS). In this case, AspRS is also charging tRNA^{Asn} with aspartic acid, yielding a mis-charged Asp-tRNA^{Asn}, which is recognized by enzymes that amidate Asp to Asn on the tRNA. The mis-charged Asp-tRNA^{Asn} does not form a stable ternary complex with EF-Tu•GTP and thus Asp is not incorporated at codons specifying Asn. This discrimination process via EF-Tu was termed thermodynamic compensation and adds to the accuracy of the translational process [82].

8.2.5

Mimicry at the Ribosomal A-site

The A-site is not restricted to binding tRNAs exclusively. During the various stages of the elongation cycle, a number of translational factors interact at the A-site. The first structures determined for these translational factors were those of EF-G [83, 84] and EF-Tu [83, 85]. Interestingly, the structure of the latter, in the form of a ternary complex EF-Tu•GTP•tRNA [86], had a striking similarity to that of EF-G•GDP, such that domains 3–5 of EF-G closely mimic the tRNA in the ternary complex (Figs. 8-6A and B; reviewed by Nissen et al. [87]). This suggested that the binding pocket of the A-site constrains the translational factors binding there to conform to a tRNA-like shape. In the last few years, solution structures for various termination factors, such

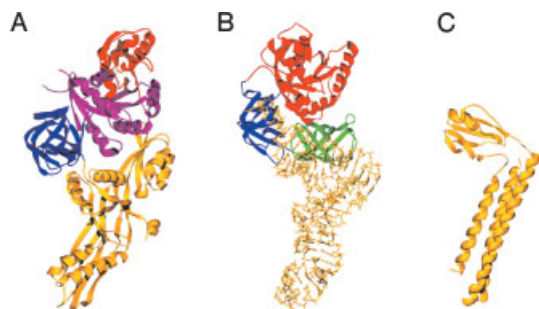


Figure 8-6 Molecular mimicry of tRNAs by translation factors. Comparison of the crystal structures for (A) EF-G GDP with domains 3–5 in gold (pdb1fmn) [148], (B) EF-Tu GTP tRNA (pdb1ttt) [86], (C) RRF (pdb1eh1) [149], figures of crystal structures were generated with Swisspdb viewer [150] and rendered with POVray.

as RF2, eRF1 and especially RRF (Fig. 8-6C) that also interact at the ribosomal A-site, have generally supported this concept. However, recent studies on the conformation and orientation of these factors on the ribosome suggest that the translation mimicry hypothesis has been over-extrapolated and that an overall tRNA shape does not necessarily suggest a binding orientation analogous to that of the tRNA (see Chap. 12 on termination for more details).

Mimicry of RNA by protein may be a more common feature in ribosomes than first realized. Organellar ribosomes generally have shorter rRNA components when compared with *E. coli*. Recent analyses of the chloroplast and mitochondrial ribosome components suggest that these rRNA losses are compensated for by both increases in size of the ribosomal protein homologs and the presence of additional organelle-specific ribosomal proteins [88–92]. Mitochondria represent an extreme example in that the protein component of the ribosomes represents two-thirds of the mass instead of one-third as in *E. coli* ribosomes. It is worth mentioning that the rRNA does consist predominantly of universally conserved residues that locate to the active centers of the ribosome, i.e., the decoding center on the 30S subunit and the PTF center on the large subunit [93], thus reinforcing the importance of these regions.

8.2.5

Translational Errors

Three types of ribosomal errors can be distinguished, the underlying mechanisms of which, not only partially overlap but are also intimately related: (i) a simple mistake in the decoding of a codon, (ii) a processivity error, and (iii) a loss of the correct reading frame (frameshift). A decoding error can lead to incorporation of an incorrect aminoacyl residue into the nascent peptide chain. A processivity error is defined as the release of a prematurely short peptidyl-tRNA from the ribosome. A shift in the

reading frame usually means the immediate loss of the genetic information, and will lead to the release of the synthesized peptide from the ribosome due to the appearance of a premature stop codon in the A-site. From the frameshift, peptide release will occur statistically within about 20 decoding steps in the incorrect reading frame since three of the 64 codons are stop codons.

Incorrect incorporation of an amino acid at a sense codon is termed a missense substitution and occurs with a global average of $\sim 3 \times 10^{-4}$ [94]. The third nucleotide of a codon is misread the most often, followed by the first one; for the decoding process the middle nucleotide of a codon seems to be the most important and is misread with the lowest detectable frequency. The codon lexicon is arranged in a way that an error in the reading of the third nucleotide of a codon results in the incorporation of either the same or a similar amino acid into the nascent chain, i.e., one with chemical properties similar to the correct amino acid such as charge or hydrophilicity. In this way, the effects of the missense substitution are buffered and usually do not lead to disastrous malfunctions of the corresponding protein. According to a rough estimate, only 1 in 400 missense events will completely inactivate the product [95].

Mis-incorporations are not only due to ribosomal decoding errors, but can be caused at the synthetase level via mis-charging. However, the charging mistakes of synthetases are usually below the level of the ribosomal mis-reading and can reach a precision of 1 mis-charging in 100 000 charging events [96]. Owing to the generally high accuracy of the synthetases, the mis-charging effects are negligible for protein synthesis (see Chap. 4 for charging mechanisms of the synthetases). EF-Tu also participates in preventing mis-incorporations in the frame of the thermodynamic compensation mechanism described in Sect. 8.2.4, whereas the discrimination cognate versus noncognate is discussed in Sect. 8.2.2 and that between cognate versus near-cognate in Sect. 8.2.3.

In the rare cases of processivity errors, a stop codon can be translated (termed readthrough) by a ternary complex aminoacyl-tRNA·EF-Tu·GTP leading to an extension on the protein product. However, usually processivity errors are premature drop-offs of the peptidyl-tRNAs, the frequency of which has been estimated to be around 4×10^{-4} (i.e., four drop-offs in 10 000 amino acid incorporations; [97]). The ester bond linking the peptidyl residue to the tRNA is more stable than the corresponding bond of an aminoacyl-tRNA. This means that peptidyl-tRNAs would accumulate in the cell over time, thereby sequestering the tRNAs and prohibitively restricting protein synthesis. Therefore, the existence of the enzyme peptidyl-tRNA hydrolase is essential for cell viability, since it cleaves the relevant ester bond (with the exceptions of fMet-tRNA and aminoacyl-tRNA), thus recycling the tRNAs. In studies with a protein of more than 1000 amino acids (β -galactosidase), the fraction of initiating ribosomes that did not complete the synthesis was estimated to $> 20\%$, and up to half of the effect was caused by a premature drop-off, the other half by truncated mRNAs resulting from an abortive transcription of the *lacZ* gene [98]. The probability of a premature drop-off is probably not identical for every codon, but is rather sensitive to context effects and occurs more often with short peptidyl-tRNAs.

Nevertheless, the energy impact of processivity errors seems to be more severe than that of missense errors, the latter being the “standard” mistake during the decoding process. An estimation of the energy loss caused by processivity errors amounts to 3% of the total energy turnover of rapidly dividing cells.

Truncated mRNA may trap a synthesizing ribosome since a stop codon necessary to provide an organized termination event is absent. Bacteria contain a stable RNA of about 350 nt that rescues these trapped ribosomes. This RNA (10Sa RNA or tmRNA) can be charged with alanine by the corresponding synthetase, occupy the A-site, and after the nascent peptide has been transferred to the alanyl residue (tRNA function) can function as a mRNA and by doing so add a 10-amino-acid peptide tag to the nascent chain, allowing an ordered termination event via a programmed stop codon. Owing to dual tRNA and mRNA functions of this RNA, it has acquired the name, tmRNA. The functions of the tmRNA are (i) to tag the abortive peptides with an additional sequence at the C-terminus that destines the peptide for efficient degradation and (ii) to recycle trapped ribosomes [99]. Although truncated mRNAs are not rare, the rescue of trapped ribosomes does – at least in some organisms – not depend solely on the presence of tmRNA, since null mutants are viable in *E. coli* although not in *Bacillus subtilis* at higher temperatures [100]. The precise mechanism of tmRNA action is not known (see Chap. 11 for more details).

What causes processivity errors to occur? Several mechanisms can cause a processivity error but the predominant cause is probably an event shortly after the onset of protein synthesis, i.e., the insertion of the growing peptide chain into the ribosomal tunnel. This tunnel can harbor a sequence of about 30 amino acids before the growing peptide chain emerges from the back of the 50S subunit into the cytosol surrounding the ribosome. The macrolide antibiotics, such as erythromycin, cause accumulation of short oligo-peptidyl-tRNAs ranging in size from 1 to 8 amino acids long depending on the macrolide (see Chap. 12). This occurs because these antibiotics, by binding within the tunnel, prevent egress of the nascent polypeptide chain and therefore induce drop-off. Another mechanism is a false stop, i.e., a sense codon is incorrectly recognized by a release factor leading to termination of protein synthesis. A false stop is a rare event with a probability of about 10^{-6} per codon [101]. Finally, frameshifts can lead to protein fragments as mentioned previously.

Since loss of the reading frame would lead to an immediate loss of the genetic information, maintaining the reading frame is an essential task of the ribosome. Usually, a loss in the reading frame occurs only once in 30 000 elongation cycles [98]; however, at the recoding site of the RF2 mRNA, where a + 1 frameshift at the 26th codon is essential for production of the full-length and active RF2 protein, loss of reading frame occurs with an efficiency of between 30 and 50%. Under certain conditions the frameshifting frequency can reach almost 100% efficiency, i.e., four orders of magnitude more often than that observed with other mRNAs. Obviously, there must be a ribosomal mechanism for maintaining the reading frame that is switched-off during RF2 synthesis. A detailed analysis has revealed that it is the presence of a cognate tRNA at the E-site that is essential for maintaining the reading frame. *In vitro* experiments show that the absence of an E-tRNA allows frameshift events to occur with a frequency of up to 20%, whereas in the presence of an E-site

tRNA no frameshifting was observed (V. Marquez, D.N. Wilson, W.P. Tate, F. Triana-Alonso and K.H. Nierhaus, in press). This does not mean that all recoding events are triggered by a pre-mature release of the E-tRNA; a detailed discussion of other aspects of recoding events can be found in Chap. 10.

8.3

The PTF Reaction

The PTF reaction is the central enzymatic activity of the large subunit. It occurs when a peptidyl-tRNA is located in the P-site and an aa-tRNA is in the A-site, termed a PRE state. Both L-shaped tRNAs at P- and A-sites form an angle of about 40° [11, 102, 23], whereas the acceptor stems are related by a translational movement, i.e. the CCA ends of both tRNAs at the PTF are related by an angle of approximate 180° and are, thus, in effect, mirror images of one another. The twist to accomplish this reflection occurs almost entirely between nucleotides 72 and 74 [103].

During PTF the α -amino group of the A-tRNA attacks the carbonyl group of the peptidyl residue of the P-tRNA, which is linked by an ester bond to the tRNA moiety (Fig. 8-7). This forms a tetrahedral intermediate, which resolves to yield a peptidyl bond. As a result, the aa-tRNA becomes a peptidyl-tRNA prolonged by one aminoacyl residue, and the former peptidyl-tRNA is stripped of its peptidyl residue to become a deacylated tRNA without a significant change of the place of the tRNA moieties [11, 104].

A long-standing debate within the translation field concerned whether or not the PTF reaction is catalyzed by proteins or rRNA. The PTF center was identified by using a putative transition state analog of the PTF reaction, which was soaked into crystals of the 50S subunit from *Haloarcula marismortui* [105]. This analog, which has been introduced by the Yarus group and hence termed the Yarus inhibitor, is a mimic of the CCA end of a P-tRNA attached to puromycin in the A-site (inset in Fig. 8-7) and is a strong competitive inhibitor of the A site substrate [106]. The region moulding the binding site of the inhibitor is densely packed with highly conserved bases of the 23S rRNA, mainly derived from the so-called PTF ring of domain V. The PTF ring structure with 41 nucleotides (Fig. 8-8) is one of the most highly conserved in rRNA, and its PTF involvement is supported by crosslinking studies from the acyl residues of tRNAs at A- and P-sites (see, e.g., Ref. [107]) as well as by mutations that render cells resistance against many antibiotics blocking peptide-bond formation (see Chap. 12 and Ref. [108] for review).

Although there are 15 proteins that interact with domain V of the 23S rRNA, only the extensions of proteins L2, L3, L4, and L10e come within 20 Å of the active site (Fig. 8-9). That the active center of the ribosome is made exclusively from RNA, implies that the ribosome is a true ribozyme.

Each of the four proteins L2, L3, L4, and L10e (a homologue of bacterial L16) has a globular domain connected to a long extension that penetrates deeply into domain V and approaches the active site. Such a long extension is quite common to ribosomal proteins and it is thought to play a role as a “glue” for the quaternary structure of the

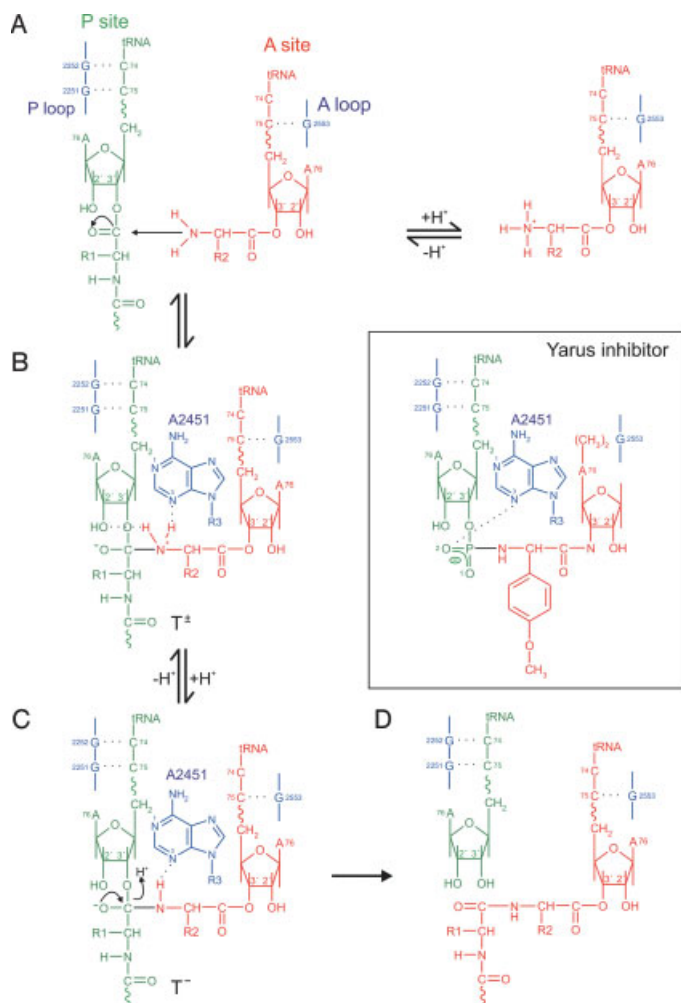


Figure 8-7 The PTF reaction. The figure shows the four possible steps of peptide-bond formation according to recent crystallographic and biochemical data [152, 103, 105, 122]. The essential features are (A) C74 and C75 of the P-site tRNA (green) are Watson–Crick paired with G2252 and G2251, respectively, of the P loop (blue). Similarly, C75 from the A-site substrate (red) forms a Watson–Crick base pair with G2553 (A-loop). The α -NH₂ function of the A-site aminoacyl-tRNA is an ammonium ion at pH 7 [153]. (B) Deprotonation of the ammonium ion triggers the nucleophilic attack of the α -amino function on the carbonyl group of the P-site substrate,

which results in the tetrahedral intermediate T_±. The secondary α -NH₂ group forms a hydrogen bond with N3 of A2451 and a second with either the 2'-OH of the A76 ribose at the P-site (shown here) or alternatively with the 2'-OH group of A2451. The oxyanion of the tetra-hedral intermediate points away from the N3-A2451 [103] and thus cannot, in contrast with the previous proposal [105], form a H-bridge. (C) Further deprotonation of the secondary α -NH₂ group leads to the tetra-hedral intermediate T⁻ and the PTF reaction is completed by an elimination step. (D) The peptidyl residue is linked to the aminoacyl-tRNA at the A-site via a peptide bond.

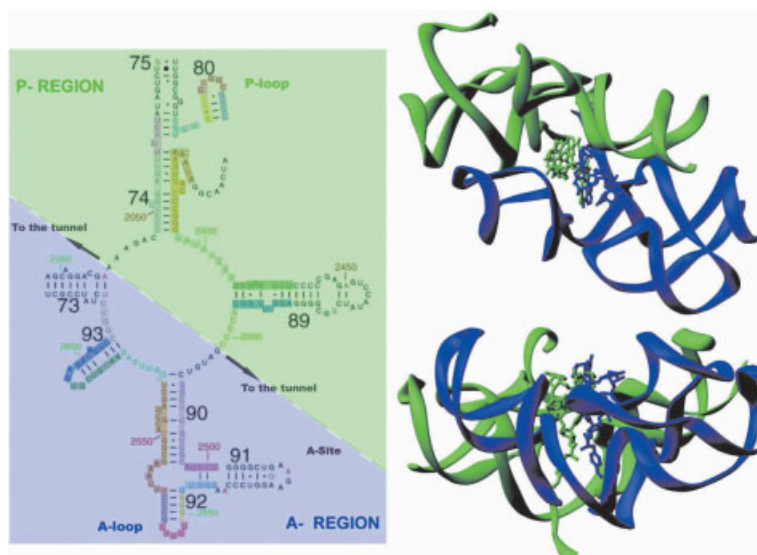


Figure 8-8 Secondary structure of the domain V of the *E. coli* 23S rRNA. Left: the A-site (blue) and P-site (green) regions that are related by 2-fold symmetry, where the symmetry-related residues within these regions are highlighted with the same color. Right: The 2-fold symmetry is illustrated from two different views using ribbon representations of the PTF center from *D. radiodurans* 50S subunit, with the A- and P-site CCA-end ligands indicated in the corresponding colors. This figure was taken from Ref. [146] with permission.

ribosome (see Chap. 1). Interestingly, three out of the four proteins in the vicinity of the PTF center are also present in eubacterial ribosomes, viz. L2, L3, and L4. These proteins have been identified previously together with 23S rRNA as major candidates for the PTF activity by single-omission tests in a total reconstitution system of the large subunit [109, 110].

One significant difference between the *Deinococcus radiodurans* 50S structure and that from *H. marismortui* is the presence of protein L27, a protein that has no homolog counterpart in the latter archaea organism [111]. L27 is one of the few proteins that are present in the interface region of the 50S subunit. It has been proposed that L27 plays a role in placement of the CCA ends of the A- and/or P-site tRNAs, and based on docking of the tRNAs from the *T. thermophilus* 70S:tRNA₃

Figure 8-7 contd. The inset is the Yarus inhibitor CCdAp-puro-mycin (CCdApPmn), which was used to identify the PTF center of the ribosome. The interactions of the Yarus inhibitor with the rRNA were deduced from 50S crystals of *H. marismortui* ribosomes after soaking the inhibitor into the crystals. Note that it was

concluded that the protonated N3 of A2451 makes a H bridge to O2, which was thought to mark the position of the oxyanion of the tetrahedral intermediate (transition state) formed during peptide-bond formation [105] (cf. with the probably correct representation in step (B).

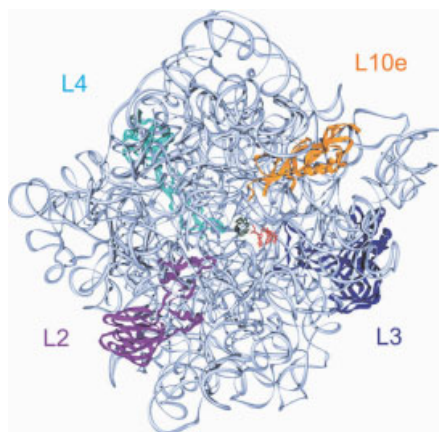


Figure 8-9 The A- and P-site products in red and green, respectively, bound at the PTF center of the 50S subunit. The proteins that reach within ~ 20 Å of the PTF center include proteins L2 (purple), L3 (blue), L4 (cyan) and L10e (brown). This figure was generated from pdb file 1KQS [25] using Swisspdb viewer [150] and rendered with POVRAY.

structure into the *D. radiodurans* 50S structure, contact of the CCA ends with L27 were predicted [111]. Indeed, photoreactive derivatives of yeast NAC-tRNA^{Phe} containing 2-azidoadenosine at their 3'-termini could be crosslinked to L27 when bound at the ribosomal P-site [112]. Recently, Zimmermann and co-workers [113] have shown that it is the very N-terminal of L27 which is crosslinked, since deletion of the 3–6 amino acids severely reduced the crosslinking efficiency and deletions of more than nine amino acids totally abolished crosslinking altogether. Therefore, L27 is more probably involved in tRNA positioning rather than in the PTF reaction itself and, furthermore, seems to be specific for only eubacteria.

The debate has now turned to whether the PTF reaction follows a physical or in addition also a chemical principle.

8.3.1

A Short Intermission: Two Enzymatic Principles of PTF Activity

There are two main principles associated with enzymatic reactions: a chemical and a physical. A number of examples exist where one or other principle is predominant but they need not be mutually exclusive (see Ref. [1] for review).

8.3.1.1 Chemical Concept: A Transient Covalent Bond between Active Center and Substrate(s)

Although the serine proteases subtilisin in bacteria and chymotrypsin in mammals have arisen independently during evolution, both have an identical activation center

for clearing the peptide bond containing a triad of Asp, His and Ser (Fig. 8-10). The three amino acid residues participate directly in the catalysis through a transient covalent event. The Asp–His module executes a general acid–base catalysis consisting of a proton donation (the acidic step), and a proton-accepting step (the basic step). The nucleophilic serine residue attacks the first substrate (which can be a peptide or an ester) forming a covalent acylated enzyme intermediate, i.e., after cleavage of the peptide bond the Ser residue binds the carbonyl residue transiently forming a seryl ester. The serine residue is then displaced via a nucleophilic attack of the second substrate (which can be an amine, a water molecule, or an alcohol). Importantly, the His residue has a pK_a of about 7, making it excellently suited to function in this type of catalysis which requires steps of both proton donation and acceptance at pH 7.

In the case of the PTF reaction, we can replace the intermediate seryl ester by a peptidyl-tRNA, where the peptidyl residue is also linked to the tRNA body via an ester bond. After nucleophilic attack by the α -amino group, a covalent intermediate is formed between the peptidyl and aa-tRNA. This intermediate complex with a tetrahedral carbon and a negatively charged oxygen is unstable and decomposes to give a peptidyl moiety (the nascent chain) linked to the aminoacyl-tRNA via a peptide bond in the A-site and a deacylated tRNA at the P-site. Both reactions occur equally well with an alcohol [114] or, with a water molecule instead of an aminoacyl-tRNA, in the case of termination reaction. The mechanism requires (i) the activation (deprotonation) of the nucleophilic α -amino group of the aa-tRNA by a general base catalyst, e.g., a His–Asp system as in the serine proteases, (ii) the stabilization of the

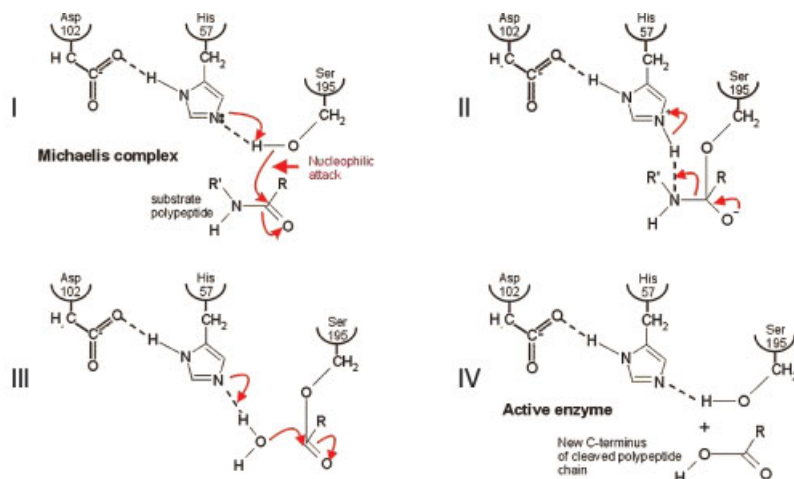


Figure 8-10 The mechanism of peptide-bond hydrolysis of serine proteases. Three amino acids Ser, His and Asp participate in this reaction. (I) The nucleophilic hydroxyl anion of the serine residue attacks the carbonyl group of the substrate (peptide bond) forming (II) a covalent

acyl-enzyme intermediate. (III) The serine molecule is then displaced via a nucleophilic attack by a water molecule. (IV) Both acyl formation and breakdown proceed via a normally high-energy tetrahedral intermediate.

tetrahedral intermediate resulting from the nucleophilic attack of the aa-tRNA on the ester linkage of peptidyl-tRNA, and (iii) the activation of the tetrahedral intermediate, which then breaks down due to proton donation from the general acid catalyst. To avoid a side reaction with a water molecule, i.e., hydrolysis of the peptidyl-tRNA during PTF reaction, the PTF center must be in a hydrophobic pocket. However, in the crystal structure of 50S (1JJ2.pdb released upon the publication of Ref. [115]) the residue A2451, which is in proximity of the PTF catalytic center (see the next section), is surrounded by 56 water molecules within a distance of 10 Å. This finding questions the assumption that the identified region for peptide-bond formation is in its fully active state, although it is competent to form a peptide bond [25].

The essential involvement of general acid–base catalysis in peptide-bond formation is consistent with the following experimental data: (i) If an enzymatic reaction is retarded in the presence of heavy hydrogen D (D₂O) instead of H (H₂O), the obvious conclusion is that a general acid–base catalysis is involved, since the migration of D versus H is slower. Precisely, such an effect has been observed for peptide-bond formation [1]. (ii) The pH dependence of peptide-bond formation peaks at pH 7, similar to the pK_a curve for a His residue [114, 116].

It was shown that the PTF activity can be blocked by His-modification reagents and that inactivation follows a one-hit kinetics of modification of His residues on 50S subunits [117], indicating that one His residue is essential for peptide-bond formation. Furthermore, phenyl-boric acid which reacts specifically with His residues, blocks peptide-bond formation [118]. Taken together, the interpretation was that a His residue might mediate a general acid–base catalysis as is known from the case of serine proteases. These suggestions of a catalytic mechanism, based on general acid–base catalysis and a possible involvement of a His residue, lead to the idea that the mechanism of serine proteases is exploited by the ribosome as well. A candidate for this His residue is His²²⁹ of L2 (see Ref. [54] for discussion and references therein). The recent X-ray analysis of 50S crystals demonstrates that a His–Asp module as in the case of serine proteases does not seem to apply, since no proteins are within 18 Å of the active site (see the next section; [105]). The role of a His residue as being seemingly critical for peptide-bond formation is therefore still unclear.

8.3.1.2 Physical Concept: The Template Model

The essence of this concept is that an enzyme organizes a defined stereochemical arrangement of the two substrates that are to be covalently bonded. The stereochemical arrangement is sufficient to allow for a dramatic acceleration of the reaction rate by 10⁶–10⁹-fold. This concept does not require any direct chemical involvement in the catalysis of the reaction such as a transient covalent binding of the substrate(s) to the enzyme.

Let us consider the acceleration factor provided by the ribosome. The upper limit of the rate for a ribosome-free environment can be estimated from a reaction between NH₂OH and AcPhe-tRNA (see Ref. [1]). The rate for the nucleophilic attack to form an ester or a peptide bond is $6 \times 10^{-5} \text{ M}^{-1} \text{ s}^{-1}$, which means one peptide bond

is formed in 30 h. On the ribosome, one peptide bond is made in 50 ms (15–20 peptide bonds per ribosome per second [119]). From these numbers $(15\text{--}20) \text{ s}^{-1}/6 \times 10^5 \text{ M}^{-1} \text{ s}^{-1}$, an acceleration factor of $3 \times 10^5 \text{ M}$ can be calculated; in other words, the ribosome accelerates the reaction by a factor of $3 \times 10^5 \text{ M}$.

Kinetic data from organic chemistry demonstrate that a rate factor of this magnitude can be obtained from simple model compounds where the reactants are appropriately juxtaposed. Bruice and Benkovic [120] have shown that the rate of intramolecular amine attack in phenyl-4(dimethylamino) butyrate (I in Fig. 8-11) is $1.3 \times 10^3 \text{ M}$ faster than bimolecular trimethylamine attack on phenyl acetate; a similar enhancement of the rate has been observed for intramolecular reaction in succinate half ester anion (II; Fig. 8-11) as compared with bimolecular reaction of acetate ion with phenyl acetate. A further rate enhancement is seen with an intramolecular reaction in the rigid ester anion (III) that proceeds 2.3×10^2 times more rapidly than that in (II), because in (III) the oxyanion nucleophile and ester are more rigidly fixed and thus better suited for the reaction, whereas (II) has rotational freedom to adopt nonproductive conformations. These results allow the prediction that if the ribosome were simply to hold the α -amino nitrogen of an aminoacyl-tRNA in the same position relative to the ester linkage of a peptidyl-tRNA as the carboxylate anion is held relative to the ester linkage in (III), peptide-bond formation would occur spontaneously with a rate comparable to the *in vivo* rate of ribosomes. The more rigid the reactants are fixed in a favorable stereochemistry, the faster the reaction proceeds. In other words, the rate of peptide-bond performance of the ribosome can be explained exclusively using the template model.

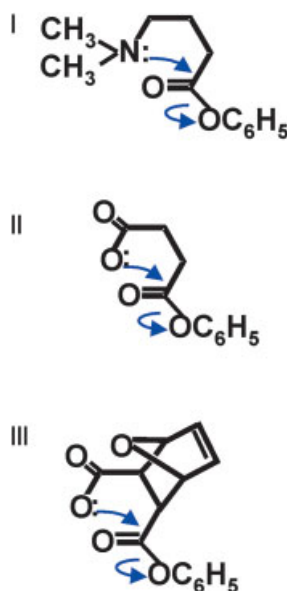


Figure 8-11 Peptide-bond formation in model compounds with appropriate juxtaposed nucleophile. See text for explanations.

8.3.2

Data from the Crystal Structures

The universally conserved residue A2451 of domain V is the nearest base to the Yarus-transition analog. It was thought to be a good candidate for a general acid–base catalyst, since its N3 is about 3 Å from the oxygen and 4 Å from the nitrogen of the phosphoamide in the Yarus inhibitor (Fig. 8-12A). This proposal was strengthened when the pK value of A2451 was found to be abnormally high at neutral pH (> 7, which is 6 pH units higher than expected) [121, 122], a property essential for acid–base catalysis as it allows for easy donation and withdrawal of a proton from the α -amino group of the aa-tRNA at the A-site. According to the same model [105], protonation of A2451 would also allow formation of a hydrogen bond with the carbonyl oxyanion of the tetrahedral transition state analog (inset of Fig. 8-7). However, the pH dependence of DMS modification at position 2451, with which the abnormally high pK of this residue was demonstrated, was subsequently shown to be displayed only by inactive ribosomes [123]. Shortly following, several groups reported that A2451 was not essential for peptide-bond formation, since ribosomes bearing mutations at position 2451 exhibited only modest (2–14-fold) decreases in the rate of peptidyl transfer [124] and were instead shown to be defective in substrate binding [125].

The next glimpse of a stage in the PTF reaction was that of the final products, obtained by soaking of A- and P-site substrates into enzymatically active *H. marismortui* 50S crystals [25]. The activity of the crystals was demonstrated by addition of the native 50S crystals to a solution containing A- and P-site substrate analogs which resulted in product formation, and ceased upon removal of the crystals. The structure determined to 2.4–3.0 Å was post-peptide-bond formation but pre-translocation and showed that the deacylated CCA bound to the P-site had its 3'-OH in close proximity to the N3 of A2451 (Fig. 8-12B) [25].

Counterevidence against the involvement of A2451 in stabilizing the transition state analog followed: If the oxyanion of the tetrahedral intermediate is hydrogen-bonded to the N3 of A2451, then this N3 must be protonated at around pH 7 and therefore should lose its proton at pH > 7.3. In this case, one would expect a strong pH dependence of the affinity of the Yarus inhibitor, since the hydrogen bond would contribute significantly to the affinity. To test this hypothesis, Strobel and co-workers [122] determined the affinity of the Yarus inhibitor for the 50S subunit at all pH values between 5 and 8.5 and found that it remained unchanged, a result inconsistent with the idea that the oxyanion is stabilized via a H-bond to the N3 of A2451. The same conclusion was drawn by subsequent crystallographic studies showing that the oxyanion of the tetrahedral intermediate points away from N3 of A2451, thus excluding a possible hydrogen bonding between these two atoms [103].

Furthermore, the Yarus inhibitor is not an honest mimic of the transition state: the distance between the O2 of the Yarus inhibitor and the 2'-C of the deoxy-A76 (dA76) ribose at the P-site is only 2.8 Å (arrowed in Fig. 8-12A). A physiological P-site substrate contains a 2'-OH at this 2'-C atom, which is essential for peptide-bond formation [126], and would sterically clash with the O2 in the position of the Yarus



rRNA are colored light blue, including the A- and P-loop bases that participate in A- and P-site CCA end fixation (*E. coli* numbering). In (B) the P-site C74 and C75 have been omitted for clarity. Dashes indicate H-bonding and rRNA nucleotides use the following color scheme: oxygen, red; phosphorus, yellow; nitrogen, blue; carbon, dark blue. (A) and (B) were generated from pdb files 1FFZ [105] and 1KQS [25], respectively, using Swisspdb viewer [150] and rendered with POVray.

inhibitor observed in the crystal. The essential nature of this 2'-OH might be explained by the observation that the α -NH₂ possibly forms a hydrogen bond with this OH (illustrated in Fig. 8-7B).

The general base catalysis debate flared up again, when Rodnina and co-workers [127] presented evidence that peptide-bond formation depends on two ionizable groups, one with a pK_a of 6.9 and the other with a pK_a of 7.5. The former was shown to be associated with the α -NH₂ group of puromycin used in the kinetic experiments, whereas the latter seemed to be ribosome-associated. The ionizable group evidently belongs to A2451 since a ribosome bearing an A2451U mutation catalyzed peptide-bond formation ~130 times slower than normal and had lost the pH dependence associated with the titratable group at a pK_a of ~7.5. However, an alternative explanation suggested by the authors was that the protonated group is part of the A2450:C2063 base pair lying directly behind A2451 (seen in Fig. 8-12B) – the candidate-ionizable group being the N1 of A2450. Although a distance of 7 Å from the N1 to the α -NH₂ group is too long for hydrogen transfer, a postulated conformational change of the PTF center might bring A2450 within the range [127]. The assumption of conformational changes broadens again the number of possible candidates that might play a role in the kind of chemical catalysis that is advocated here. We note that evidence has been presented implicating His²²⁹ of protein L2 in this catalysis [54], although current maps place this residue more than 20 Å from the tetrahedral intermediate of the transition state. The best that can be said at the moment is that a direct role of A2451 in a general acid–base catalysis is hard to be reconciled with the observation that A2451 in active ribosomes does not contain a titratable group at this pK_a in contrast with inactive ribosomes [123].

In fact, the ribosome need not directly involve chemically in the catalysis of the PTF reaction, such as the formation of a transient covalent interaction between the substrate (tRNAs) and the enzyme (the ribosome or, more specifically, in this case the rRNA). The template model predicts that tight stereochemical arrangement of substrates relative to one another would be sufficient to provide the dramatic acceleration of the reaction rate needed for peptide-bond formation (see the previous section). In this case, the role of A2451 would be to withdraw a proton from free nucleophilic α -NH₂ group of the A-site substrate or form a hydrogen bond with the α -NH₂ group, thus promoting peptide-bond formation via proper positioning of the NH₂ group. The reaction scheme would follow similar to that presented in Fig. 8-7 and described in more detail in the corresponding legend.

Tight fixation of the CCA ends of the P- and A-tRNAs is exactly what is observed both in the analog soaked 50S crystal structure (Fig. 8-12A) and also with the 50S structure containing the products of the PTF reaction following soaking of the A- and P-site substrates (Fig. 8-12B). In the P-site, the CCA end is locked into position by two Watson–Crick base pairs, viz. C74 and C75 with G2252 and G2251. A76 stacks on the ribose of A2451 (seen clearly in Fig. 8-12B). In the A-site, the CCA end of the aa-tRNA is fixed by (i) Watson–Crick base-pairing between C75 and G2553, (ii) a type-I A-minor motif between A76 and the G2583–U2506 base pair, and (iii) an additional H-bond interaction between the 2'-OH of A76 with U2585. Tight fixation

of the CCA ends of both A- and P-tRNAs at the PTF center underlines the importance of the template model in peptide-bond formation, viz. that precise stereochemical fixation is predominantly responsible for the enormous acceleration of the reaction. The rate of peptide-bond formation on the ribosome of $\sim 50 \text{ s}^{-1}$ was estimated to be $\sim 10^5$ faster than the uncatalyzed reaction (the rate in the absence of ribosomes) [1]. The PTF reaction without chemical catalysis (i.e., ribosomal ionizing group is protonated at $\text{pH} < 7$) occurs with a rate of $\sim 0.5 \text{ s}^{-1}$ [127], which is still >1000 faster than the uncatalyzed reaction. If this estimation is correct then the physical mode of peptide-bond formation represents approximately 90% of the reaction rate, with the chemical mode making up the remaining 10%.

8.3.3

Why both the Physical and Chemical Concepts for Peptide-bond Formation?

If the physical mode sufficiently explains the overall rate of protein synthesis, why does the chemical mode exist in addition? A possible explanation is that the template model requires a maximal rigid surface for the ligands, whereas the ribosome has to be flexible to allow the movement of the $\text{mRNA} \cdot \text{tRNA}_2$ complex during translocation. To achieve both a fast rate and a flexible structure of the ribosome, both physical and chemical catalysis might need to be involved for an optimal rate of protein synthesis, although it is already clear that the template (physical) mode probably plays the dominant role in peptide-bond formation.

8.4

The Translocation Reaction

Following peptide-bond formation, the positions of the tRNAs remain unchanged. This has been demonstrated by cryo-EM analyses of *E. coli* ribosome complexes [11, 104] and – concerning the CCA ends at the PTF center – by soaking A- and P-site substrates into active 50S *H. marismortui* crystals and solving the structure of the reaction products after peptide-bond formation [25]. Now the ribosome must transfer the products, the peptidyl-tRNA in the A-site and deacylated tRNA in the P-site, to the P- and E-sites respectively, i.e., shifting the ribosome from PRE to POST state (Figs. 8-1(c) and (f), respectively). This process is termed translocation. It must be extremely accurate at both ends of the tRNA molecule: the anticodon–codon complex must be moved exactly 10 \AA (the length of one codon), longer or shorter movements will change the reading frame. At the other end of the A-site peptidyl-tRNA, the CCA end must also be precisely moved into the P-site so as to set up the next peptidyl-transferase reaction with the incoming A-tRNA. Incorrect placement of the peptidyl-tRNA at the P-site could be disastrous for peptide-bond formation and lead to abortion of translation.

Ribosomes have an innate translocase activity [14], but it is more than one order of magnitude slower than that of the EF-G catalyzed reaction [13]. This implies that the structures necessary to move the tRNAs reside in the ribosome and that the role of

EF-G (and EF2 in eukaryotes) is to reduce the activation energy barrier that separates the two sets of tRNA positions. Important questions remaining unanswered are: How does EF-G mediate translocation and what ribosomal components are involved in transfer of the tRNAs?

8.4.1

Conservation in the Elongation Factor-G Binding Site

The crystal structure of EF-G has been solved in the nucleotide-free form [83] and in complex with GDP [84]. The GTP form is the active one, which binds to the ribosome and triggers translocation. Hydrolysis of GTP inactivates EF-G and dissociates it from the ribosome (reviewed in Ref. [128]). EF-G belongs to the same subfamily of G proteins as IF2, RF3, and EF-Tu, the latter of which has been crystallized in both GTP (active) and GDP (inactive) forms. Comparison of these EF-Tu structures reveals that they exhibit large domain shifts relative to one another [85].

Cryo-EM reconstructions of EF-G bound to bacterial 70S ribosomes at 17.5–20 Å [7, 129, 9] and EF2 to eukaryotic 80S ribosomes at 17.5 Å [130] show similar binding sites for both factors (Figs. 8-13A and B). In these complexes, antibiotics were used

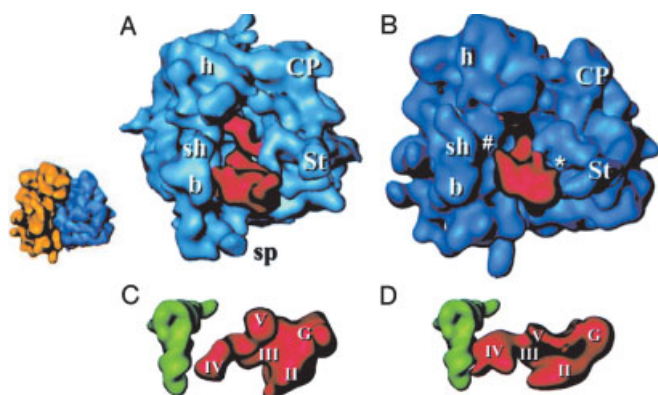


Figure 8-13 Comparison of cryo-electron microscopic analyses of EF-G 70S complex from *E. coli* and EF2 80S complex from *S. cerevisiae*. Side view of (A) EF-G 70S complex and (B) EF2 80S complex with small subunit on left and large subunit on right. The same orientation is seen, in the small inset on the left, of an empty 80S ribosome, where the 40S and 60S subunits are colored yellow and blue, respectively. Relative arrangements of (C) EF-G and P-tRNA and (D) EF2 and P-tRNA (where the P-tRNA was placed into the 80S density map on the basis of the position observed in a P-tRNA-bound 70S ribosome reconstruction). Landmark abbreviations are for the small subunit: b, body; bk, beak; h, head; sh, shoulder and sp, spur. Landmarks for the large subunit: CP, central protuberance; St, L7/L12 stalk. The roman numerals on EF-G/EF2 refer to the domains. Figures modified from Gomez-Lorenzo et al. [130].

to trap the elongation factor on the ribosome. EF-G was trapped on the 70S ribosome using the antibiotic fusidic acid, which allows translocation and GTP hydrolysis, but blocks the switch into the GDP conformer of the factor, preventing dissociation from the ribosome. The eukaryotic eEF2 was locked on the yeast ribosome using the antifungal sordarin, which is thought to function analogously to fusidic acid [130]. The EF-G complex was formed with a typical PRE state, i.e., A- and P-tRNAs were present. As expected, the tRNAs were translocated to the P- and E-sites, but of special interest is that the tip, domain IV, of EF-G was shown to occupy the position of the A-site. Similarly, the position for EF2 seen in the EF2:ribosome complex also occupied the A-site, and came very close to the position of the P-tRNA (Figs. 8-13C and D). EF-G-mediated translocation is also possible in the presence of nonhydrolyzable GTP analogs, such as GDPNP, thus suggesting that binding of EF-G alone is sufficient for translocation and that hydrolysis is necessary for conformational change and release of EF-G-GDP [128]. We repeat that the fact that translocation is an intrinsic activity of the ribosome has been shown by the factor free “spontaneous” translocation [131]. Furthermore, a dipeptidyl-tRNA that has been formed at the A-site via peptide-bond formation shows a much faster spontaneous translocation than a chemically made dipeptidyl-tRNA that has been bound to the A-site [13]. The energy for translocation therefore might arise by the peptide-bond formation, at least in part. The surprising observation that the antibiotic sparsomycin, an efficient blocker of peptide-bond formation, is able to effectively trigger a single translocation has corroborated the view that it is not the energy from the EF-G-dependent GTP hydrolysis that drives the translocation [132].

Precisely the opposite view, namely that EF-G-dependent GTP hydrolysis limits the translocation reaction thus accelerating the translocation, has been put forward by one group [37]. In this case, EF-G would be considered a “motor protein”, although this view has not yet been accepted by the wider scientific community. One reason might be that the same group has published just the opposite results about 15 years ago: Also applying stop-flow measurements, they showed that the translocation reaction limits the EF-G-dependent GTP hydrolysis and not *vice versa*, namely that EF-G-dependent GTP cleavage occurs *after* translocation and thus the correspondingly released energy cannot directly flow into the translocation reaction [34].

For classical G-proteins, a GTPase-activating protein (GAP) stimulates the G-protein-mediated hydrolysis of GTP. In the case of EF-G/EF2, the GAP is provided by components of the ribosome. There are certainly gross conformational changes visible upon binding of each elongation factor to the ribosome. One of the most striking changes is seen within the stalk region; density for this region is absent in the empty 70S and 80S ribosomes but becomes more ordered upon EF-G/EF2 binding [7, 129, 130], supporting its universal role in factor binding. The best candidates for the GAP role include the pentameric stalk complex, which consists of the ribosomal proteins L10 (L7/L12)₄, as well as a region of the 23S rRNA termed the sarcin-ricin loop (SRL). The SRL is so named because cleavage after G2661 of the bacterial 23S rRNA within this region by the highly specific RNase α -sarcin inhibits all elongation

factor-dependent activities [133] and similar effects are seen after removing the neighboring base A2660 (*E. coli* nomenclature) in the 26S rRNA of yeast by the N-glycosidase activity of the ricin A-chain [134]. Furthermore, this region contains the longest (12 nucleotides) universally conserved stretch of rRNA underlining its functional importance. Recently, hybrid ribosomes were constructed where the proteins at the GTPase center from *E. coli*, L7/L12 and L10, were replaced with their eukaryotic counterparts from rat P1/P2 and P0, respectively [135]. Both the *in vitro* translation and GTPase activity of the resultant hybrid ribosomes were strictly dependent on the presence of the eukaryotic elongation factors, EF2 and EF1a. This reflects not only the specificity of the interaction between the stalk proteins and the elongation factors from each kingdom, but also the importance of the stalk proteins in mediating elongation factor GTPase activity.

The ribosomal protein L11 (and associated L11-binding site of the 23S rRNA) is often considered as a candidate for a GAP role and is often referred to as the GTPase-associated center (GAC) alone and collectively with the SRL (however to avoid confusion we will refrain from using this term, especially since L11 is unlikely to be a true GAC of the ribosome, see following). The reason that L11 has been assigned a GAP role is because mutations in both L11 and its binding site on the 23S rRNA can confer resistance against the antibiotic thiostrepton, a potent inhibitor of EF-G- and EF-Tu-dependent GTPase activities [136]. However, the direct involvement of L11 in the factor-dependent GTPase is not very probable, since (i) mutants lacking L11 are viable, although extremely compromised as indicated by about 6-fold growth retardation [137], and (ii) the IF-2-dependent GTPase is stimulated rather than blocked by thiostrepton [138]. Furthermore, replacement of either the L10 (L7/L12)₄ complex or L11 with the equivalent rat protein showed that the P0 (P1 P2)₂ complex, but not the eukaryotic counterpart to L11 (RL12), was responsible for factor specificity and associated GTPase dependence, although addition of L11 or RL12 did stimulate protein synthesis significantly [135]. Consistently, L11 is certainly in close proximity to the elongation factors: cryo-EM analyses of EF-G bound to 70S ribosomes revealed that upon binding of EF-G, the N-terminal domain of L11 is shifted so as to form an arc-like connection with the G-domain of EF-G [139]. This arc-like connection is also observed in the EF2–80S complex although it is broader and more fused [130]. However, from cryo-EM reconstructions of EF-Tu ternary complex ribosome complexes stalled with the antibiotic kirromycin, it is the α -sarcin/ricin loop that makes direct contact with the G domain of the EF-Tu [104] and not the L11 region. Although residue 1067 within H43 of the L11-binding site rRNA makes definite contact with the highly conserved region of the T arm of the tRNA, no contact between L11 and the tRNA is observed in the recent 9 Å reconstruction [104], in contrast with earlier proposals that were based on lower resolution reconstructions [140]. The most striking result to emerge from the improved resolution was an observed movement of 7 Å in the L11 region upon ternary complex binding to bring this region into contact with the tRNA [104]. This leads the authors to propose a model, whereby the conformation change in the L11 region perturbs the orientation of the tRNA such that codon–anticodon interaction can be established,

which in turn provides the trigger for GTPase activation of EF-Tu. In this model, the L11 region would not act as a GAP directly, but would stimulate the activity consistent with the available biochemical data.

Lastly, it is noteworthy that L11 also stimulates the stringent response factor RelA in the presence of a deacylated tRNA at the ribosomal A-site, which leads to the RelA-dependent synthesis of (p)ppGpp, an essential effector during the stringent response (see Chap. 11).

8.4.2

Dynamics within the Ribosome

The α - ε model for translocation hypothesizes a moveable domain within the ribosome that carries the A- and P-tRNAs during translocation (reviewed in Ref. [43]). Evidence for this model comes from testing the accessibility of phosphate groups on the tRNAs in the PRE and POST states. The essential observation was that the protection patterns of A- and P-tRNAs differ from one another, but the corresponding tRNAs exhibit the same protection patterns in the PRE state as they do in the POST. This suggests that distinct ribosomal components are involved in carrying the tRNAs from the PRE to the POST state. In contrast with the intensive contact patterns observed with tRNAs bound to programmed ribosomes, the 40 nucleotides of mRNA covered by the ribosome [141] have almost no specific contacts with the ribosome, except two positions upstream of the two decoding codons (i.e., those codons involved in codon–anticodon interactions; [142]). This immediately suggests that the tightly bound tRNAs are the handle to move the tRNA₂•mRNA complex during translocation, whereas the mRNA follows because of the direct connection with the tRNAs via the two adjacent codon–anticodon interactions. This is one important reason why the two adjacent tRNAs maintain their simultaneous codon–anticodon interaction before (A- and P-sites) and after translocation (P- and E-sites).

There are a number of candidates that may play a role in translocation of the tRNAs or even constitute portions of the moveable domains. Distinct regions within the crystal structures are disordered, most probably reflecting flexibility in these components. A classic example is the stalk region, which, as already mentioned, only becomes ordered upon factor binding. Another is the L1 region, the flexibility of which may regulate E-tRNA release. There are also certain structures that become either ordered or rearranged upon subunit association. Most of these elements are constituents of intersubunit bridges. One striking example is the universally conserved H69 in domain IV of the large subunit rRNA. H69 is the major element of bridge B2a, the largest intersubunit bridge (see Fig. 8-14), and is disordered in the *H. marismortui* 50S subunit structure but ordered in the *D. radiodurans* 50S subunit. Comparing the latter structure with the *T. thermophilus* 70S structure suggests that upon association H69 swings out towards h44, another very flexible element. In this extended conformation, H69 would be predicted to make contact with both A- and P-tRNAs [111]. Another element that is not fully resolved in either of the 50S structures is H38 of domain II, a constituent of bridge B1a, often called the “A-site

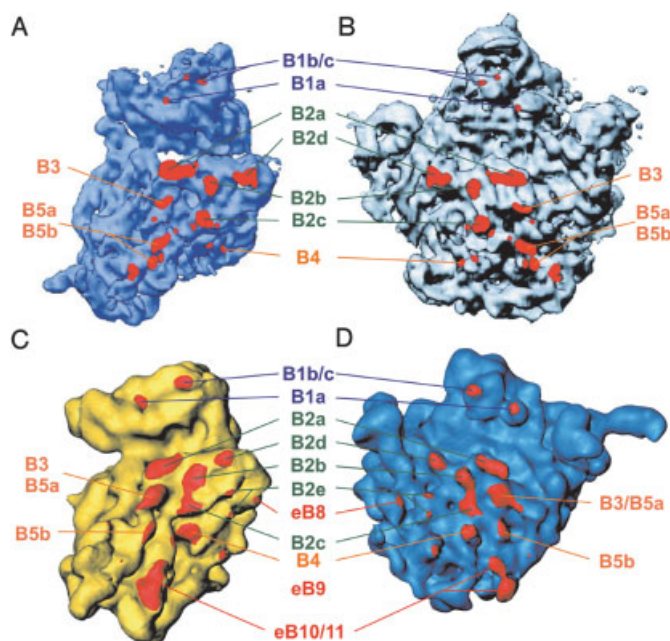


Figure 8-14 Comparison of intersubunit bridge positions between bacteria and yeast ribosomes. (A, B): The 30S (blue) and 50S (gray) ribosomal subunits of *T. thermophilus* are shown from their intersubunit sides. Intersubunit bridges are marked in red and are annotated according to the nomenclature from Gabashvili et al. [52], where the lettering of the bridges B1, B2 and B3–B5 are labeled in blue, green and orange, respectively. Figure adapted from Cate et al. [154]. (C, D): The 40S (yellow) and 60S (blue) ribosomal subunits of *S. cerevisiae* are also shown from the interface side with the intersubunit bridges in red. The lettering common to *T. thermophilus* are labeled in blue (B1), green (B2) and orange (B3–B5), whereas those of additional intersubunit connections in the yeast ribosome are labeled eB8–eB11 in red. Note that bridges B6 and B7 are not included for simplicity. Adapted from Spahn et al. [155].

finger” because it contacts the A-tRNA. As previously mentioned, both B1a and B2a bridge elements have corresponding counterparts within the 80S yeast ribosome, strengthening their candidacy for a role in translocation.

The most significant progress of our understanding of the translocation reaction comes from a detailed cryo-EM study of this reaction [31], together with a biochemical analysis [143]. EF-G induces a ratchet-like movement of the 30S subunits as first shown with empty ribosomes [144], but here the movement could be coupled with translocation of tRNAs at higher resolution, yielding further insight into this reaction: EF-G•GTP does not bind to ribosomes in a POST state or to ribosomes that

carry a peptidyl-tRNA at the P-site, but does so with high affinity if the ribosome carries only a deacylated tRNA at the P-site as it is the case in the PRE state after peptide-bond formation (see Fig. 8-2B). However, it is difficult to imagine how EF-G binding is influenced by a deacylated tRNA at the P-site, when the A-site is occupied with a peptidyl-tRNA.

The former state is denoted “locked” for binding of EF-G•GTP, the latter “unlocked”, although no structural differences could be detected at the resolution of 10–13 Å. The following picture emerged: (i) After occupying the A-site with an aa-tRNA and peptide-bond formation, the peptidyl-tRNA is in the A-site and a deacylated tRNA at the P-site, no hybrid site is visible. (ii) EF-G•GTP binds and induces the first forth-movement of the ratchet motion of the 30S subunit, a turn of about 20°. During this movement, the deacylated tRNA is seen in a hybrid position P/E and it is believed (although not yet observed) that the peptidyl-tRNA would also occupy a hybrid position A/P. (iii) The ribosome triggers the EF-G-dependent GTP hydrolysis and the authors postulate that the resulting EF-G conformational change into the GDP conformer completes the translocation reaction in that (i) the 30S subunit moves back (second part of the ratchet movement), (ii) the tRNAs continue their movement to E- and P-sites, respectively, and (iii) EF-G•GDP dissociates from the ribosome. Until now, EF-G•GTP has not been successfully crystallized, whereas EF-G•GDP has. A comparison of the structure of EF-G•GDPNP (a GTP analog) on the ribosome with that of the crystallized EF-G•GDP revealed a striking shift of domains 3–5 resulting in a movement of about 35 Å of the tip of domain 4. The authors postulated that this dramatic movement, similar in extent to that observed between the GTP and GDP conformers of EF-Tu (40 Å), promotes the back movement of the ratchet motion and might be also essential for the release of EF-G•GDP from the ribosome. If the striking conformational change is causing the release of EF-G rather than the second half of the ratchet movement, then the EF-G-dependent GTP hydrolysis has nothing to do with a motor protein function of this elongation factor. If, however, the GTP hydrolysis is in fact promoting the back-swing of the 30S subunit, then this could be interpreted as the molecular-correlate to a motor-protein role of EF-G. The authors [31] also detect a substantial movement of the L1 protuberance during the translocation and postulate an active participation of this structure in the translocation of the deacylated tRNA from the P-site to the E-site.

During the translocation reaction a movement of a peptidyl-tRNA from the A-site to the P-site via a P/E hybrid position can be easily reconciled with the α - ε model as has been suggested previously [51]. Note the difference to the hybrid-site model. This model postulates that after peptide-bond formation and before translocation the tRNAs move on the large subunit but stay on the 30S subunit, i.e., the peptidyl-tRNA at the A-site moves from A/A-site to the A/P-site, and only the translocation movement brings the tRNA into the P/P-site. In contrast, the cryo-EM study suggests that during translocation the peptidyl-tRNA moves from the A- to the P-site via a transient A/P position.

Despite the asymmetry of the ribosome, an internal symmetry within the large ribosomal subunit has been identified ([145]; reviewed in Refs. [146, 147]). The fact

that the CCA ends of tRNAs at the A- and P-sites are related by 180° rotation rather than by a translational movement like the rest of the tRNA [103, 105, 25], suggested that at least a minimum of symmetry might exist within the PTF center of the ribosome. However, Yonath and co-workers [145] realized that this symmetry extended beyond the A and P loops, and identified two regions of approximately 90 nucleotides that are related by rotational symmetry in the *D. radiodurans* 50S subunit (Fig. 8-8). The closest residues to the center of rotation include a number of residues of the PTF ring, strands of H89 and H93 and the stem loops of H92 and H80, which are the A and P loops, respectively (symmetry-related residues are colored with corresponding colors in Fig. 8-8). A similar symmetry was also discovered within the large subunit from archaea *H. marismortui* and thermophilic eubacteria *T. thermophilus* suggesting that it is a conserved feature of ribosomes. This is in itself not surprising since this region of the ribosome is highly conserved, but does add an extra dimension. But what is the significance of the symmetry?

Following peptide-bond formation, the peptidyl-ACC of the A-site tRNA must move into the P-site of the PTF center, i.e., a transition from making interactions with the A loop to making interactions with the P loop. Since the symmetry-related residues within the PTF center effectively provide a lining for the walls of the cavity, the idea arose that the CCA ends of the tRNA should follow a rotation movement during translocation. By computational modelling of such a transition, it was possible to accomplish a rotation from the A- to the P-site without any steric clashes. Interestingly, the symmetry-related residues within the P-site are located slightly deeper in the tunnel than the corresponding A-site residues, leading to the proposal that the rotational movement during translocation drives the peptide into the tunnel [147].

One of the most exciting discoveries related to the rotational symmetry was that the motion is centered on residue A2602. This residue is known to be highly flexible, a fact emphasized by the different orientation of the adenine base of this residue in almost all the different crystal structure complexes solved to date. Indeed, upon binding of many ligands, such as antibiotics and CCA-end mimics, A2602 assumed a different position [146]. This flexibility and the location of A2602 at the center of rotation may suggest that A2602 has a role in guiding the CCA end of the tRNA from the A- to the P-site. Another conserved residue predicted to maintain interaction throughout the rotational motion was U2585, which has also been identified as being very flexible.

The ribosome research is in exciting upheaval phase where the structure begins to explain the function. For the first time, we can imagine how the ribosome is using its complicated structure to perform its complicated function.

References

- 1 K. H. Nierhaus, H. Schulze, B. S. Cooperman, *Biochem. Int.* **1980**, *1*, 185–192.
- 2 K. H. Nierhaus, *Angew. Chem. Int. Ed.* **1996**, *35*, 2198–2201.
- 3 K. H. Nierhaus: in *Ribosomal RNA and Group I Int*, eds R. Green, R. Schroeder, R. G. Landes, Georgetown, TX 1996, 69–81.
- 4 K. H. Nierhaus: in *Nature Encyclopedia of Life Sciences*, Nature Publishing Group, London 1999, www.els.net.
- 5 D. N. Wilson, G. Blaha, S. R. Connell et al., *Curr. Protein Pept. Sci.* **2002**, *3*, 1–53.
- 6 D. N. Wilson, K. H. Nierhaus, *Angew. Chem. Int. Ed. Engl.* **2003**, *42*, 3464–3486.
- 7 R. Agrawal, P. Penczek, R. Grassucci et al., *Proc. Natl. Acad. Sci. USA* **1998**, *95*, 6134–6138.
- 8 H. Stark, E. V. Orlova, J. Rinke-Appel et al., *Cell* **1997**, *88*, 19–28.
- 9 H. Stark, M. V. Rodnina, H. J. Wieden et al., *Cell* **2000**, *100*, 301–309.
- 10 M. Valle, J. Sengupta, N. K. Swami et al., *EMBO J.* **2002**, *21*, 3557–3567.
- 11 R. K. Agrawal, C. M. T. Spahn, P. Penczek et al., *J. Cell. Biol.* **2000**, *150*, 447–459.
- 12 S. Schilling-Bartetzko, A. Bartetzko, K. H. Nierhaus, *J. Biol. Chem.* **1992**, *267*, 4703–712.
- 13 K. Bergemann, K. H. Nierhaus, *J. Biol. Chem.* **1983**, *258*, 15105–15113.
- 14 L. P. Gavrilova, A. S. Spirin, *FEBS Lett.* **1971**, *17*, 324–326.
- 15 A. R. Cukras, D. R. Southworth, J. L. Brunelle et al., *Mol. Cell* **2003**, *12*, 321–328.
- 16 U. R. Kutay, C. M. T. Spahn, K. H. Nierhaus, *Biochim. Biophys. Acta* **1990**, *1050*, 193–196.
- 17 J. R. Mesters, A. P. Potapov, J. M. de Graaf et al., *J. Mol. Biol.* **1994**, *242*, 644–654.
- 18 A. Savelsbergh, V. I. Katunin, D. Mohr et al., *Mol. Cell* **2003**, *11*, 1517–1523.
- 19 J. M. Berg, J. L. Tymoczko, L. Stryer: *Biochemistry*, 5th edition, Freeman, New York 2002.
- 20 F. J. Triana-Alonso, K. Chakraborty, K. H. Nierhaus, *J. Biol. Chem.* **1995**, *270*, 20473–20478.
- 21 H. R. Bourne, D. A. Sanders, F. McCormick, *Nature* **1990**, *348*, 125–132.
- 22 D. Moazed, H. F. Noller, *Nature* **1989**, *342*, 142–148.
- 23 M. M. Yusupov, G. Z. Yusupova, A. Baucom et al., *Science* **2001**, *292*, 883–896.
- 24 H. F. Noller, M. M. Yusupov, G. Z. Yusupova et al., *FEBS Lett.* **2002**, *514*, 11–16.
- 25 T. M. Schmeing, A. C. Seila, J. L. Hansen et al., *Nat. Struct. Biol.* **2002**, *9*, 225–230.
- 26 Y. Semenov, T. Shapkina, V. Makhno et al., *FEBS Lett.* **1992**, *296*, 207–210.
- 27 D. Moazed, H. F. Noller, *Cell* **1989**, *57*, 585–597.
- 28 A. Gnirke, K. H. Nierhaus, *J. Biol. Chem.* **1986**, *261*, 14506–14514.
- 29 H. J. Rheinberger, K. H. Nierhaus, *J. Biomol. Struct. Dyn.* **1987**, *5*, 435–446.
- 30 R. K. Agrawal, P. Penczek, R. A. Grassucci et al., *J. Biol. Chem.* **1999**, *274*, 8723–8729.
- 31 M. Valle, A. Zavialov, J. Sengupta et al., *Cell* **2003**, *114*, 123–134.
- 32 C. M. Spahn, G. Blaha, R. K. Agrawal et al., *J. Mol. Cell.* **2001**, *7*, 1037–1045.
- 33 J. M. Robertson, H. Paulsen, W. Wintermeyer, *J. Mol. Biol.* **1986**, *192*, 351–360.
- 34 J. M. Robertson, C. Urbanke, G. Chinali et al., *J. Mol. Biol.* **1986**, *189*, 653–662.
- 35 J. Wadzack, N. Burkhardt, R. Jünemann et al., *J. Mol. Biol.* **1997**, *266*, 343–356.
- 36 J. Remme, T. Margus, R. VILLEMS et al., *Eur. J. Biochem.* **1989**, *183*, 281–284.
- 37 M. V. Rodnina, A. Savelsbergh, V. I. Katunin et al., *Nature* **1997**, *385*, 37–41.

- 38 H.-J. Rheinberger, K. H. Nierhaus, *Proc. Natl. Acad. Sci. USA* **1983**, 80, 4213–4217.
- 39 H.-J. Rheinberger, K. H. Nierhaus, *J. Biol. Chem.* **1986**, 261, 9133–9139.
- 40 A. Gnirke, U. Geigenmüller, H.-J. Rheinberger et al., *J. Biol. Chem.* **1989**, 264, 7291–7301.
- 41 T. P. Hausner, U. Geigenmüller, K. H. Nierhaus, *J. Biol. Chem.* **1988**, 263, 13103–13111.
- 42 H. Saruyama, K. H. Nierhaus, *Mol. Gen. Genet.* **1986**, 204, 221–228.
- 43 K. H. Nierhaus, C. M. T. Spahn, N. Burkhardt et al., in *The Ribosome. Structure, Function, Antibiotics, and Cellular Interactions*, eds R. A. Garrett, S. R. Douthwaite, A. Liljas et al., ASM Press, Washington, DC 2000, 319–335.
- 44 R. A. Grajevskaja, Y. V. Ivanov, E. M. Saminsky, *Eur. J. Biochem.* **1982**, 128, 47–52.
- 45 H.-J. Rheinberger, H. Sternbach, K. H. Nierhaus, *Proc. Natl. Acad. Sci. USA* **1981**, 78, 5310–5314.
- 46 H.-J. Rheinberger, H. Sternbach, K. H. Nierhaus, *J. Biol. Chem.* **1986**, 261, 9140–9143.
- 47 U. Geigenmüller, K. H. Nierhaus, *EMBO J.* **1990**, 9, 4527–4533.
- 48 M. Dabrowski, R. Junemann, M. A. Schäfer et al., *Biochemistry (Moscow)* **1996**, 61, 1402–1412.
- 49 M. Dabrowski, C. M. T. Spahn, M. A. Schäfer et al., *J. Biol. Chem.* **1998**, 273, 32793–32800.
- 50 N. Polacek, S. Patzke, K. H. Nierhaus et al., *Mol. Cell* **2000**, 6, 159–171.
- 51 M. A. Schäfer, A. O. Tastan, S. Patzke et al., *J. Biol. Chem.* **2002**, 277, 19095–19105.
- 52 I. S. Gabashvili, R. K. Agrawal, C. M. T. Spahn et al., *Cell* **2000**, 100, 537–549.
- 53 M. S. VanLoock, R. K. Agrawal, I. S. Gabashvili et al., *J. Mol. Biol.* **2000**, 304, 507–515.
- 54 G. Diedrich, C. M. T. Spahn, U. Stelzl et al., *EMBO J.* **2000**, 19, 5241–5250.
- 55 R. Willumeit, S. Forthmann, J. Beckmann et al., *J. Mol. Biol.* **2001**, 305, 167–177.
- 56 H. Bertschold, L. Reshetnikova, C. O. A. Reiser et al., *Nature* **1993**, 365, 368.
- 57 N. Bilgin, L. A. Kirsebom, M. Ehrenberg et al., *Biochimie* **1988**, 70, 611–618.
- 58 G. Blaha, K. H. Nierhaus, *Cold Spring Harbor Symposia on Quantitative Biology*, **2001**, 135–145 Vol. 65.
- 59 H. Echols, M. F. Goodman, *Annu. Rev. Biochem.* **1991**, 60, 477–511.
- 60 R. T. Libby, J. L. Nelson, J. M. Calvo et al., *EMBO J.* **1989**, 8, 3153–3158.
- 61 K. Beebe, L. Ribas De Pouplana, P. Schimmel, *EMBO J.* **2003**, 22, 668–675.
- 62 A. C. Bishop, K. Beebe, P. R. Schimmel, *Proc. Natl. Acad. Sci. USA* **2003**, 100, 490–494.
- 63 T. L. Hendrickson, T. K. Nomanbhoy, V. de Crecy-Lagard et al., *Mol. Cell* **2002**, 9, 353–362.
- 64 K. H. Nierhaus, *Mol. Microbiol.* **1993**, 9, 661–669.
- 65 H. Stark, M. V. Rodnina, H. J. Wieden et al., *Nat. Struct. Biol.* **2002**, 15, 15–20.
- 66 A. Weijland, A. Parmeggiani, *Science* **1993**, 259, 1311–1314.
- 67 N. Bilgin, M. Ehrenberg, C. Kurland, *FEBS Lett.* **1988**, 233, 95–99.
- 68 A. P. Potapov, *FEBS Lett.* **1982**, 146, 28–33.
- 69 A. P. Potapov, F. J. Triana-Alonso, K. H. Nierhaus, *J. Biol. Chem.* **1995**, 270, 17680–17684.
- 70 J. M. Ogle, D. E. Brodersen, W. M. Clemons Jr et al., *Science* **2001**, 292, 897–902.
- 71 S. Osawa, T. H. Jukes, K. Watanabe et al., *Microbiol. Rev.* **1992**, 56, 229–264.
- 72 J. M. Ogle, F. V. Murphy, M. J. Tarry et al., *Cell* **2002**, 111, 721–732.
- 73 A. P. Carter, W. M. Clemons, D. E. Brodersen et al., *Nature* **2000**, 407, 340–348.
- 74 W. M. Clemons, J. L. C. May, B. T. Wimberly et al., *Nature* **1999**, 400, 833–840.
- 75 K. H. Nierhaus, *Biochemistry* **1990**, 29, 4997–5008.

- 76 J. J. Hopfield, *Proc. Natl. Acad. Sci. USA* **1974**, *71*, 4135–4139.
- 77 J. Ninio, *Biochimie* **1975**, *57*, 587–595.
- 78 M. Ehrenberg, D. Andersson, K. Mohman et al.: in *Structure, Function and Genetics of Ribosomes*, eds B. Hardesty, G. Kramer, Springer, New York 1986, 573–585.
- 79 M. V. Rodnina, T. Daviter, K. Gromadski et al., *Biochimie* **2002**, *84*, 745–754.
- 80 S. Schilling-Bartetzko, F. Franceschi, H. Sternbach et al., *J. Biol. Chem.* **1992**, *267*, 4693–4702.
- 81 A. M. Karim, R. C. Thompson, *J. Biol. Chem.* **1986**, *261*, 3238–3243.
- 82 F. J. LaRiviere, A. D. Wolfson, O. C. Uhlenbeck, *Science* **2001**, *294*, 165–168.
- 83 A. Aevansson, E. Brazhnikov, M. Garber et al., *EMBO J.* **1994**, *13*, 3669–3677.
- 84 J. Czworkowski, J. Wang, T. A. Seitz et al., *EMBO J.* **1994**, *13*, 3661–3668.
- 85 H. Berchtold, L. Reshetnikova, C. O. A. Reiser et al., *Nature* **1993**, *365*, 126–132.
- 86 P. Nissen, M. Kjeldgaard, S. Thirup et al., *Science* **1995**, *270*, 1464–1472.
- 87 P. Nissen, M. Kjeldgaard, J. Nyborg, *EMBO J.* **2000**, *19*, 489–495.
- 88 K. Yamaguchi, K. von Knoblauch, A. R. Subramanian, *J. Biol. Chem.* **2000**, *275*, 28455–28465.
- 89 E. C. Koc, W. Burkhardt, K. Blackburn et al., *J. Biol. Chem.* **2001**, *276*, 19363–19374.
- 90 E. C. Koc, W. Burkhardt, K. Blackburn et al., *J. Biol. Chem.* **2001**, *276*, 43958–43969.
- 91 T. Suzuki, M. Terasaki, C. Takemoto-Hori et al., *J. Biol. Chem.* **2001**, *276*, 33181–33195.
- 92 K. Yamaguchi, A. R. Subramanian, *J. Biol. Chem.* **2000**, *275*, 28466–28482.
- 93 M. R. Sharma, E. C. Koc, P. P. Datta et al., *Cell* **2003**, *115*, 97–108.
- 94 F. Bouadloun, D. Donner, C. G. Kurland, *EMBO J.* **1983**, *2*, 1351–1356.
- 95 J. Langridge, J. H. Campbell, *Mol. Gen. Genet.* **1969**, *103*, 339–347.
- 96 F. Cramer, U. Englisch, W. Freist et al., *Biochimie* **1991**, *73*, 1027–1035.
- 97 J. R. Menninger, *J. Biol. Chem.* **1976**, *251*, 3392–3398.
- 98 F. Jorgensen, C. G. Kurland, *J. Mol. Biol.* **1990**, *215*, 511–521.
- 99 K. C. Keiler, P. R. H. Waller, R. T. Sauer, *Science* **1996**, *271*, 990–993.
- 100 A. Fujihara, H. Tomatsu, S. Inagaki et al., *Genes Cells* **2002**, *7*, 343–350.
- 101 F. Jorgensen, F. M. Adamski, W. P. Tate et al., *J. Mol. Biol.* **1993**, *230*, 41–50.
- 102 K. H. Nierhaus, J. Wadzack, N. Burkhardt et al., *Proc. Natl. Acad. Sci. USA* **1998**, *95*, 945–950.
- 103 J. L. Hansen, T. M. Schmeing, P. B. Moore et al., *Proc. Natl. Acad. Sci. USA* **2002**, *99*, 11670–11675.
- 104 M. Valle, A. Zavialov, W. Li et al., *Nat. Struct. Biol.* **2003**, *10*, 899–906.
- 105 P. Nissen, J. Hansen, N. Ban et al., *Science* **2000**, *289*, 920–930.
- 106 M. Welch, J. Chastang, M. Yarus, *Biochemistry* **1995**, *34*, 385–390.
- 107 G. Steiner, E. Kuechler, A. Barta, *EMBO J.* **1988**, *7*, 3949–3955.
- 108 C. M. T. Spahn, C. D. Presscott, *J. Mol. Med.* **1996**, *74*, 423–439.
- 109 F. Franceschi, K. H. Nierhaus, *J. Biol. Chem.* **1990**, *265*, 16676–16682.
- 110 H. Schulze, K. H. Nierhaus, *EMBO J.* **1982**, *1*, 609–613.
- 111 J. Harms, F. Schlutzenzen, R. Zarivach et al., *Cell* **2001**, *107*, 679–688.
- 112 S. Kirillov, J. Wower, S. Hixson et al., *FEBS Lett.* **2002**, *514*, 60–66.
- 113 B. Maguire, A. Beniaminov, P. Ramu et al.: in *8th Annual Meeting of the RNA Society*, RNA Society, Vienna **2003**, 199.
- 114 S. R. Fahnestock, H. Neumann, V. Shashua et al., *Biochemistry* **1970**, *9*, 2477–2483.
- 115 D. J. Klein, T. M. Schmeing, P. B. Moore et al., *EMBO J.* **2001**, *20*, 4214–4221.
- 116 B. E. Maden, R. E. Monro, *Eur. J. Biochem.* **1968**, *6*, 309–316.

- 117 K. K. Wan, N. D. Zahid, R. M. Baxter, *Eur. J. Biochem.* **1975**, *58*, 397–402.
- 118 I. Rychlik, J. Cerna, *Biochem. Int.* **1980**, *1*, 193–200.
- 119 H. Bremer, P. P. Dennis: in *Escherichia coli and Salmonella*, eds F. C. Neidhardt, R. C. III, J. L. Ingraham, et al., ASM Press, Washington, DC 1996, 1553–1569.
- 120 T. Bruice, S. Benkovic, *J. Am. Chem. Soc.* **1963**, *85*.
- 121 G. W. Muth, L. Ortoleva-Donnelly, S. A. Strobel, *Science* **2000**, *289*, 947–950.
- 122 K. M. Parnell, A. Seila, S. A. Strobel, *Proc. Natl. Acad. Sci. USA* **2002**, *99*, 11658–11663.
- 123 M. A. Bayfield, A. E. Dahlberg, U. Schulmeister et al., *Proc. Natl. Acad. Sci. USA* **2001**, *98*, 10096–10101.
- 124 J. Thompson, D. F. Kim, M. O'Connor et al., *Proc. Natl. Acad. Sci. USA* **2001**, *98*, 9002–9007.
- 125 N. Polacek, M. Gaynor, A. Yassin et al., *Nature* **2001**, *411*, 498–501.
- 126 K. Quiggle, G. Kumar, T. W. Ott et al., *Biochemistry* **1981**, *20*, 3480–3485.
- 127 V. I. Katunin, G. W. Muth, S. A. Strobel et al., *Mol. Cell* **2002**, *10*, 339–346.
- 128 Y. Kaziro, *Biochim. Biophys. Acta* **1978**, *505*, 95–127.
- 129 R. K. Agrawal, A. B. Heagle, P. Penczek et al., *Nat. Struct. Biol.* **1999**, *6*, 643–647.
- 130 M. G. Gomez-Lorenzo, C. M. T. Spahn, R. K. Agrawal et al., *EMBO J.* **2000**, *19*, 2710–2718.
- 131 L. P. Gavrilova, A. S. Spirin: in *Methods in Enzymology*, eds K. Moldave and L. Grossmann, vol. 30 1974, 452–462.
- 132 K. Fredrick, H. F. Noller, *Science* **2003**, *300*, 1159–1162.
- 133 T. P. Hausner, J. Atmadja, K. H. Nierhaus, *Biochimie* **1987**, *69*, 911–923.
- 134 Y. Endo, K. Tsurugi, *J. Biol. Chem.* **1987**, *262*, 8128–8130.
- 135 T. Uchiumi, S. Honma, T. Nomura et al., *J. Biol. Chem.* **2002**, *277*, 3857–3862.
- 136 E. Cundliffe: in *The Ribosome: Structure, Function and Evolution*, eds W. E. Hill, A. Dahlberg, R. A. Garrett et al., ASM Press, Washington, DC 1990, 479–490.
- 137 G. Stöffler, E. Cundliffe, M. Stöffle-Meilicke et al., *J. Biol. Chem.* **1980**, *255*, 10517–10522.
- 138 D. M. Cameron, J. Thompson, P. E. March et al., *J. Mol. Biol.* **2002**, *319*, 27–35.
- 139 R. K. Agrawal, J. Linde, J. Sengupta et al., *J. Mol. Biol.* **2001**, *311*, 777–787.
- 140 H. Stark, M. V. Rodnina, J. Rinkeappell et al., *Nature* **1997**, *389*, 403–406.
- 141 D. Beyer, E. Skripkin, J. Wadzack et al., *J. Biol. Chem.* **1994**, *269*, 30713–30717.
- 142 E. V. Alexeeva, O. V. Shpanchenko, O. A. Dontsova et al., *Nucleic Acids Res.* **1996**, *24*, 2228–2235.
- 143 A. V. Zavialov, M. Ehrenberg, *Cell* **2003**, *114*, 113–122.
- 144 J. Frank, R. K. Agrawal, *Nature* **2000**, *406*, 318–322.
- 145 A. Bashan, I. Agmon, R. Zarivach et al., *Mol. Cell* **2003**, *11*, 91–102.
- 146 I. Agmon, T. Auerbach, D. Baram et al., *Eur. J. Biochem.* **2003**, *270*, 2543–2556.
- 147 A. Bashan, R. Zarivach, F. Schlutzenzen et al., *Biopolymers* **2003**, *79*, 19–41.
- 148 M. Laurberg, O. Kristensen, K. Martemyanov et al., *J. Mol. Biol.* **2000**, *303*, 593–603.
- 149 T. Toyoda, O. F. Tin, K. Ito et al., *RNA* **2000**, *6*, 1432–1444.
- 150 N. Guex, M. C. Peitsch, *Electrophoresis* **1997**, *18*, 2714–2723.
- 151 U. B. Rawat, A. V. Zavialov, J. Sengupta et al., *Nature* **2003**, *421*, 87–90.
- 152 R. Green, J. R. Lorsch, *Cell* **2002**, *110*, 665–668.
- 153 J. M. Berg, J. R. Lorsch, *Science* **2001**, *291*, 203.
- 154 J. H. Cate, M. M. Yusupov, G. Z. Yusupova et al., *Science* **1999**, *285*, 2095–2104.
- 155 C. M. Spahn, R. Beckmann, N. Eswar et al., *Cell* **2001**, *107*, 373–386.